STRUCTURAL PRINCIPLES OF GIANT CELLS

Sten Samson

Gates and Crellin Laboratories of Chemistry,*

California Institute of Technology, Pasadena, California

INTRODUCTION

It is a curious coincidence that the paper by Linus Pauling,[1] which first described the crystal structure of an intermetallic compound, presented simultaneously one of the most complicated structure problems that lay ahead. In this paper Pauling discussed the atomic arrangement of Mg_2Sn, which has the calcium fluoride structure, and also gave a brief account of an X-ray diffraction study of crystals of $NaCd_2$. The diffraction patterns of these crystals were so complicated, however, that it was not then possible to assign indices with certainty to many of the spots. The unit of structure was later[2] reported to be a cube that has an edge length slightly over 30Å and contains about 384 sodium atoms and 768 cadmium atoms. The space group is $Fd3m$ (O_h^7). Thus, we see that the existence of this most complex compound has been known for 45 years, ever since the first structure determination of an intermetallic compound was published.

A compound with structure apparently similar to that of $NaCd_2$ is βMg_2Al_3. Cursory investigations[3,4] of small crystal fragments were found to represent a cubic structure, space group $Fd3m(O_h^7)$, with approximately 1166 atoms per unit cube of edge length a_o = 28.22Å.

Observation of powder diffraction patterns led to the conclusion[5] that βMg_2Al_3 is isomorphous with Cu_4Cd_3. This phase can be

*Contribution No. 3585.

B. C. Giessen (ed.), *Developments in the Structural Chemistry of Alloy Phases*

obtained only after prolonged annealing and forms through a solid-state reaction of a metastable eutectic mixture of the two phases $CdCu_2$ ($C36$ type[6,7]) and Cd_8Cu_5 ($D8_2$ type[8]), that always seem to precipitate first on solidification of the melt. It is, therefore, difficult to grow crystals of this compound. When single crystals were finally obtained after extremely long periods of annealing, they were found, indeed, to be cubic,[9] but the X-ray diffraction patterns turned out to be drastically different from those of $NaCd_2$ and βMg_2Al_3. A cursory investigation[9] showed that the probable space group is $F\bar{4}3m(T_d^2)$, $F432(O^3)$, or $Fm3m(O_h^5)$ with approximately 1116 atoms per unit cube of edge $a_o = 25.87$Å. This work was completed recently.[6] The final results obtained correspond to one formula unit of $Cu_{640}Cd_{484}$ per unit cube of space group $F\bar{4}3m$.

Up to the present $NaCd_2$, βMg_2Al_3, and Cu_4Cd_3 have seemed to exhibit the largest structural units that have been observed in intermetallic compounds. These units, containing more than 1100 atoms each, are referred to here as the "giant cells".

It is possible that more compounds of comparable or even greater complexity exist, but that, as yet, these have escaped my detection. I should welcome any information or suggestions as to the likelihood of this.

The reason for interest in these complex structures is that they incorporate a large number of crystallographically independent coordination shells and hence represent a valuable source of information with regard to the atomic configurations that lead to maximum stability.

THE MOST IMPORTANT COORDINATION POLYHEDRA OBSERVED IN COMPLEX METALLIC STRUCTURES

The description of crystal structures, in which all the atoms are arranged so as to fill space, as is the case in intermetallic compounds, is virtually a portrayal of the configuration of atoms around single atoms. In some cases, the configurations can be described conveniently by reference to the five regular polyhedra. In the majority of cases, however, one has to resort to polyhedra of a more complicated geometrical nature. These are cumbersome to describe in the course of a structure study and are therefore discussed separately in the following sections. Some configurations have been given short names: each name refers to the metallic phase in which the configuration was first discovered. In the interest of brevity, the word ligancy (L) is used throughout instead of coordination number (CN).

The Friauf Polyhedron (Ligancy 16)

This polyhedron can be derived through relatively simple modifications of the cubic closest-packed arrangement of spheres of equal size (face-centered cube). A configuration of sixteen such spheres is shown in Fig. 1a. Removal of a tetrahedron of four contiguous spheres from this aggregate results in the framework of twelve spheres (called B spheres), arranged about the corners of a truncated tetrahedron, as shown in Fig. 1b. The central cavity is

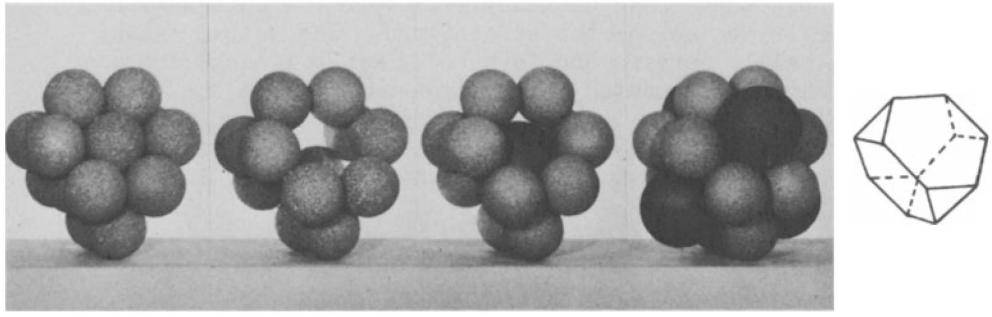

a b c d e

Figure 1. To derive the Friauf polyhedron from an aggregate of sixteen spheres of equal size arranged in the cubic closest packing. (a) The group of sixteen spheres. (b) and (c) The truncated tetrahedron. (d) The aggregate of seventeen spheres referred to as the Friauf polyhedron. (e) A formal representation of the Friauf polyhedron. Here, the atoms out from the centers of the hexagons are not indicated for reasons explained in the text.

capable of accommodating a thirteenth sphere (called A sphere) with a radius 1.35 times that of the surrounding spheres, as shown in Fig. 1c. Out from the center of each of the four hexagons there is an additional sphere of the large kind (up to 35 per cent larger in radius), as shown in Fig. 1d. The central (large) sphere, accordingly, is surrounded by sixteen spheres, twelve small and four large ones.

This group of seventeen spheres is called a Friauf polyhedron, since it was first discovered in the Friauf phases $MgCu_2$[10] and $MgZn_2$.[11] It consists, as we see, of two integral parts: (1) the truncated (say, positive) tetrahedron bounded by four hexagons and

four triangles (twelve vertices); (2) the regular (negative) tetrahedron (four vertices, representing four large atoms).

In the formal representation of the Friauf polyhedron shown in Fig. 1e, the spheres out from the centers of the hexagons forming the regular, negative tetrahedron are not indicated, since, in most instances, each such sphere is shared between two adjacent Friauf polyhedra or between a Friauf polyhedron and a different kind of coordination shell. The reader should be alerted to the fact that in subsequent discussions reference will be made sometimes to the Friauf polyhedron and sometimes to the truncated tetrahedron, and that these two terms have distinctly different meanings although they may refer to one and the same figure. The actual Friauf polyhedron has 16 corners and is bounded by 28 triangular faces although only the truncated tetrahedron is shown in the figures.

Figure 2 shows a layer of truncated tetrahedra arranged so as to fill a plane. Each such tetrahedron shares three of its four

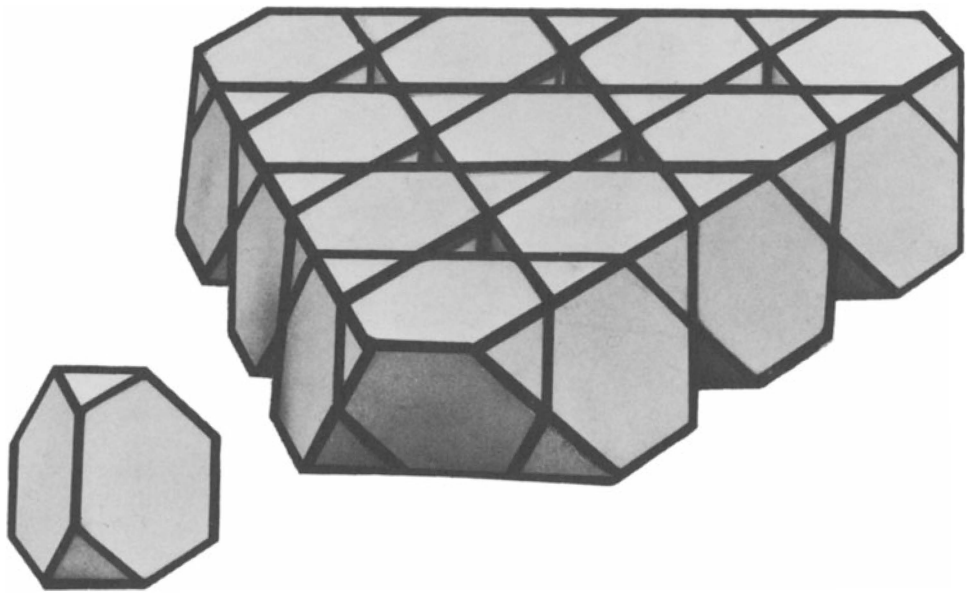

Figure 2. A close-packed layer of truncated tetrahedra forming Friauf polyhedra.

hexagons with three other polyhedra; the unshared fourth hexagon may be shared by a truncated tetrahedron of the next layer that may be superimposed on this one. It is seen that then each large atom, called A, out from the center of a hexagon represents, in turn, the center of an adjacent Friauf polyhedron.

A geometrical feature of close-packed, regular truncated tetrahedra of edge length a is that the center-to-center distance (A-A) becomes 1.23 × a, whereas the center-to-vertex distance (A-B) is 1.17 × a. With twelve contiguous spheres of radius 0.5 a (B spheres) at the vertices, the truncated tetrahedron can accommodate a central sphere (A sphere) of radius (1.17 - 0.5)a = 0.67a, whereas in the close-packed layer the A-A distance corresponds to a radius of only (0.5 × 1.23)a = 0.615a, which is 8 per cent shorter.

The Friauf polyhedra observed in the three structure types C14 ($MgZn_2$[11]), C15 ($MgCu_2$[10]), and C36 ($MgNi_2$[12]) are very nearly of this kind, and hence, exhibit metrical properties that are clearly inconsistent with spherically shaped atoms. It seems that the A atoms are elongated in the directions of the twelve A-B bonds and shortened in the directions of the four tetrahedral A-A bonds. In fact, the A atoms would seem to have a tetrahedral shape if the B atoms were spherical. Probably, neither A nor B is spherical.

The μ-Phase Polyhedron (Ligancy 15)

The twelve spheres of equal size shown in Fig. 3a are arranged about the vertices of a truncated trigonal prism bounded by eight triangles (four above and four below; see also Figs. 3d,e) and three hexagons. The central cavity of this framework is capable of accommodating a thirteenth sphere of radius, about 1.31 times that of the surrounding spheres, as shown in Fig. 3b. Out from the center of each of the three hexagons there is an additional sphere of the large kind, as shown in Fig. 3c. The central large sphere, accordingly, is surrounded by fifteen spheres, twelve small (called B) and three large ones (called A).

This group of atoms was first observed in the μ phases W_6Fe_7, W_6Co_7, Mo_6Fe_7, and Mo_6Co_7[13] and is therefore referred to as the μ-phase polyhedron.

A formal representation of this polyhedron is shown in Figs. 3d,e. Again, the atoms out from the centers of the hexagons are not shown, since, in most cases, each such atom is shared between two adjacent μ-phase polyhedra or between a μ-phase polyhedron and a different kind of coordination shell with which it shares its hexagon.

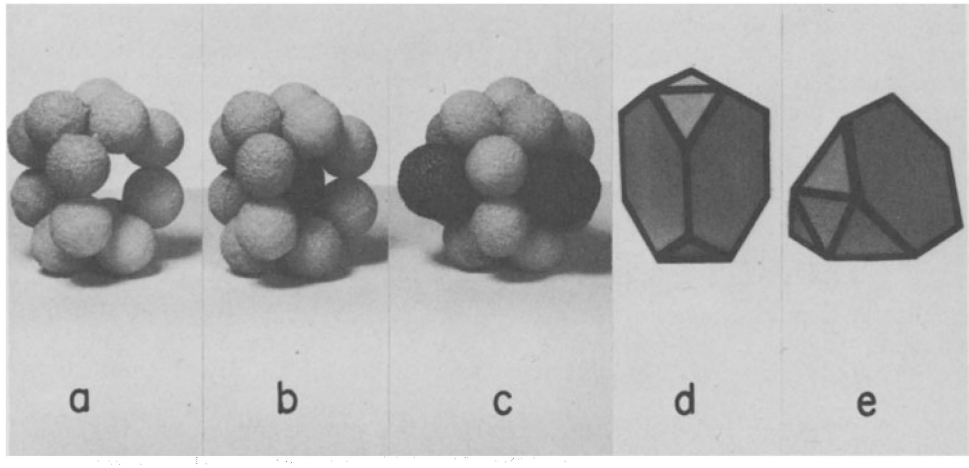

Figure 3. (a) Twelve spheres of equal size are arranged about the vertices of a truncated trigonal prism. (b) The central cavity is appropriate for a thirteenth sphere of radius 1.31 times that of the surrounding ones. (c) Three more large spheres are added to form the μ-phase polyhedron of L15. (d) and (e) A formal representation of the μ-phase polyhedron: here the atoms out from the hexagons are not indicated.

In the μ phases[13] these polyhedra are arranged so as to fill a plane, as is shown in Fig. 4. It is of interest to note that here the center-to-center distance between adjacent truncated trigonal prisms (sharing hexagons) is exactly the same as the center-to-vertex distance (if they were regular polyhedra), which is $(2/\sqrt{3})\cdot a = 1.155a$. If, again, twelve contiguous B spheres of radius 0.5a (one-half the edge length of the truncated prism) were at the vertices, the center-to-vertex distance would correspond to a central sphere of radius $(1.155 - 0.5)a = 0.655a$, whereas the center-to-center distance (A-A distance) corresponds to a radius of only $(0.5 \times 1.155)a = 0.578a$, which is nearly 12 per cent shorter. Thus, it seems that each A atom (large atom at the center) is elongated in the directions of the twelve A-B bonds and shortened in the directions of the three trigonal A-A bonds. In fact, each A atom appears to be trigonally deformed, even if the B atoms were assumed to be spherical. However, in reality, it is highly unlikely that either A or B is spherical.

Again, the reader should be alerted to the fact that only the truncated trigonal prism will be shown in subsequent figures, although the term μ-phase polyhedron refers to the coordination shell that has 15 corners and 24 triangles.

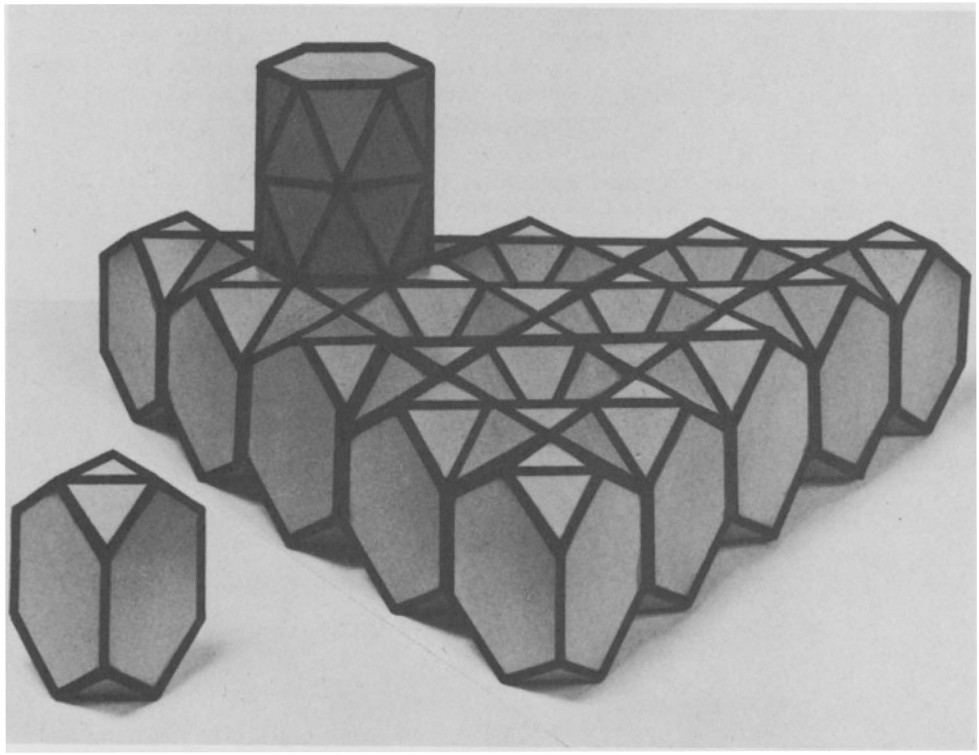

Figure 4. Arrangement of μ-phase polyhedra so as to fill a plane.

The Hexagonal Prism and Antiprism with Two Atoms at the Extended Poles (Ligancy 14)

A considerable number of the coordination shells of ligancy 14 observed in intermetallic compounds belong to this group.

The regular hexagonal prism with square prism faces, having eighteen edges (excluding poles) of length a corresponds to a center-to-vertex distance of $a \cdot \sqrt{5}/2 = 1.118a$ and, accordingly, is appropriate for the accommodation of a central sphere which has a radius of 0.618a, which is 1.236 times that of the twelve surrounding spheres of radius 0.5a.

Conversion of a hexagonal prism (plus two atoms at the extended poles, L14) into an antiprism leads to an increase in the number of edges from 30 to 36, and the six square prism faces are replaced by twelve triangles. Addition of spheres out from the centers of square prism faces gives rise to octahedral interstices, whereas

the triangles of the antiprisms lead to the creation of tetrahedral interstices and, thus, to a reduction of the interstitial space. This may be one of the reasons why hexagonal antiprisms are much more frequently observed in metallic structures than are hexagonal prisms. The hexagonal antiprism, which has two atoms at the extended poles, has 14 corners and is bounded by 24 triangles.

In most cases the two hexagons of each antiprism differ in size; usually the larger hexagon has all or part of its corners occupied by large atoms, the smaller by small atoms. In cases where these antiprisms are arranged so as to form a close-packed layer (Fig. 5) the side of each large hexagon is $2/\sqrt{3} = 1.155$ times that of the small one.

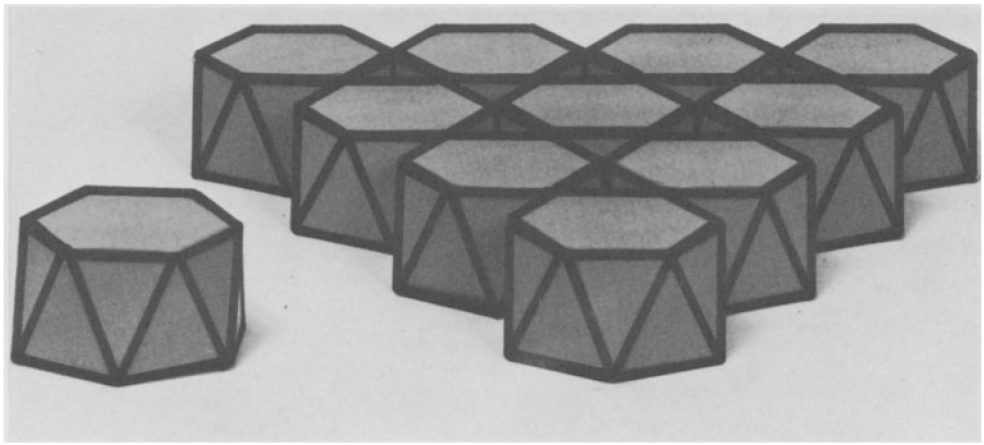

Figure 5. Hexagonal antiprisms arranged so as to form a close-packed layer. The side of each large hexagon is $2/\sqrt{3}$ times that of each small hexagon.

Frequently, two antiprisms share a large hexagon and thus form a bi-antiprism (μ phase[13], P phase[14]); see also Figs. 7 and 8. A close-packed layer of such complexes is observed in the μ-phase structure; see Fig. 6. The hexagonal bi-antiprism referred to here is not to be confused with the coordination shell of ligancy 18 observed in the $D2_d$ ($CaCu_5$) type of structure, in which the central atom is at the center of the large hexagon.

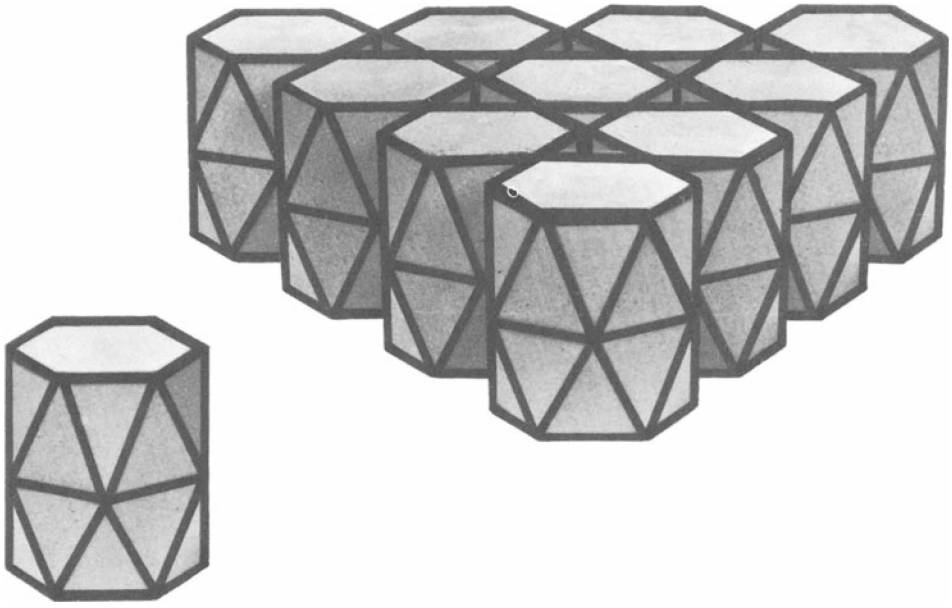

Figure 6. Two close-packed layers of hexagonal antiprisms, in which each large hexagon is shared by the lower and the upper layers, as is the case in the μ-phase structure.

Each atom at the extended pole of an antiprism is surrounded usually by a μ-phase polyhedron, a Friauf polyhedron, or, in turn, by an antiprism (Figs. 6, 7, 8).

The Friauf polyhedron (L16), the μ-phase polyhedron (L15), and the hexagonal antiprism (plus two atoms at the poles, L14) are related to each other as follows: The Friauf polyhedron can be described as a hexagonal antiprism which has one atom out from the center of the small hexagon and three atoms that form a triangle out from the center of the large hexagon. The μ-phase polyhedron is obtained through replacement of these three atoms by two atoms.

The Cubo-Octahedron, the Icosahedron, and the Pentagonal Prism with Two Atoms at the Poles (Ligancy 12)

The icosahedron can be derived through relatively simple modifications of the cubo-octahedron (which is observed in the cubic closest-packed structures). Figure 9a shows fourteen spheres arranged at the lattice points of a face-centered cube.

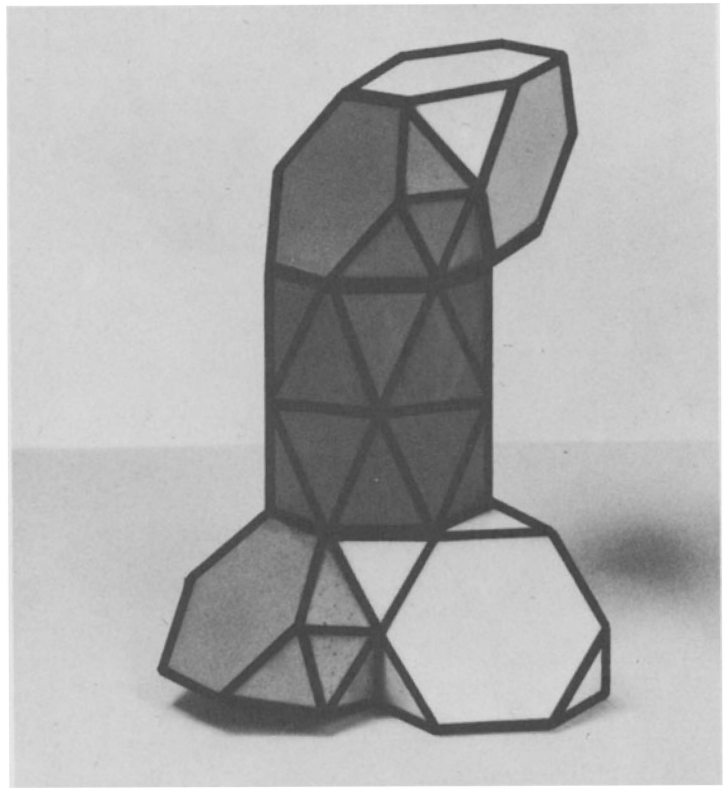

Figure 7. The sequence of contiguous polyhedra as observed in the P(Mo-Ni-Cr) phase: μ-phase polyhedron, Friauf polyhedron, hexagonal bi-antiprism, μ-phase polyhedron, Friauf polyhedron ···. The zigzag chain is of infinite length.

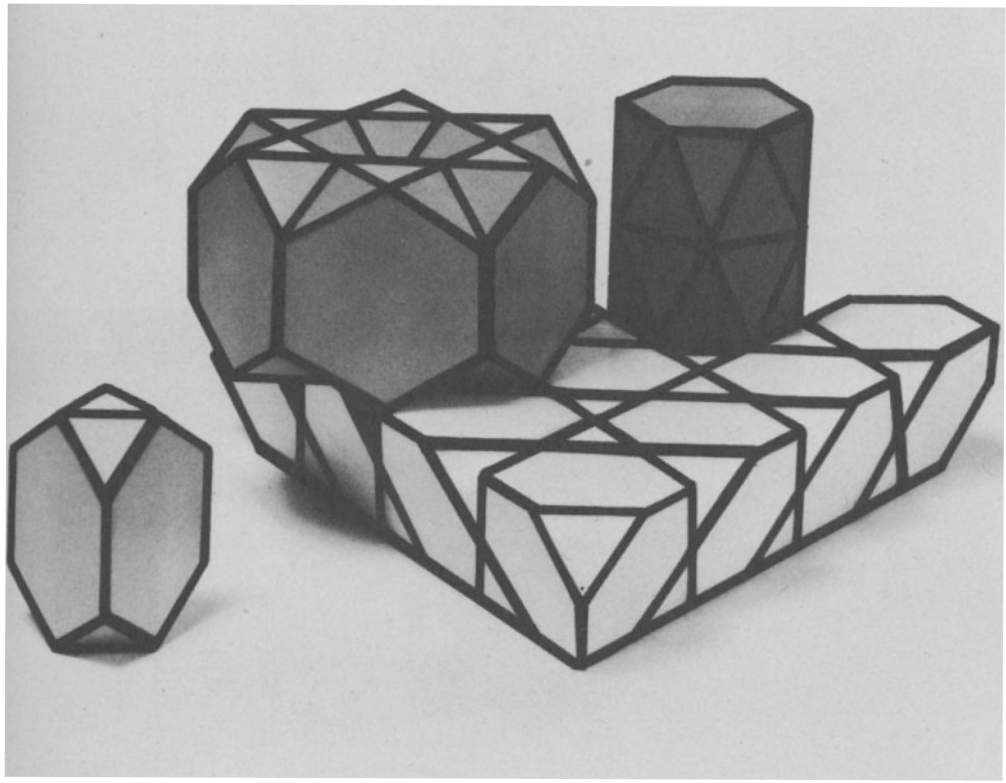

Figure 8. A layer of Friauf polyhedra in which the horizontal triangles are shared with μ-phase polyhedra, and the hexagons with hexagonal antiprisms. A set of six contiguous μ-phase polyhedra is shown to the left, a hexagonal bi-antiprism (right) is created by each such sixfold set.

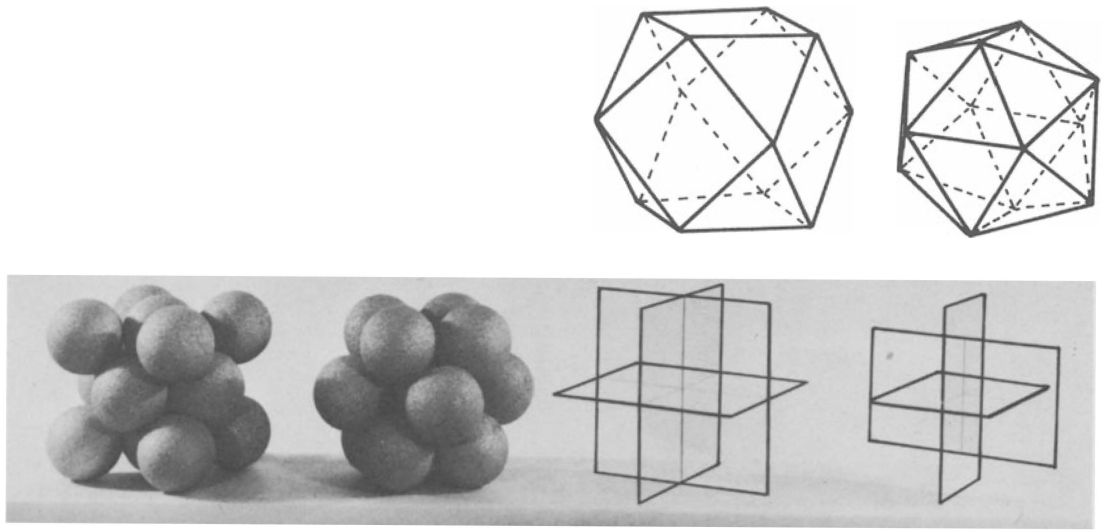

Figure 9. The group of twelve spheres at the vertices of the cubo-octahedron shown in (b) is brought into view by translation of the origin of the face-centered cube shown in (a). The cubo-octahedron is shown in (c) and the icosahedron in (d).

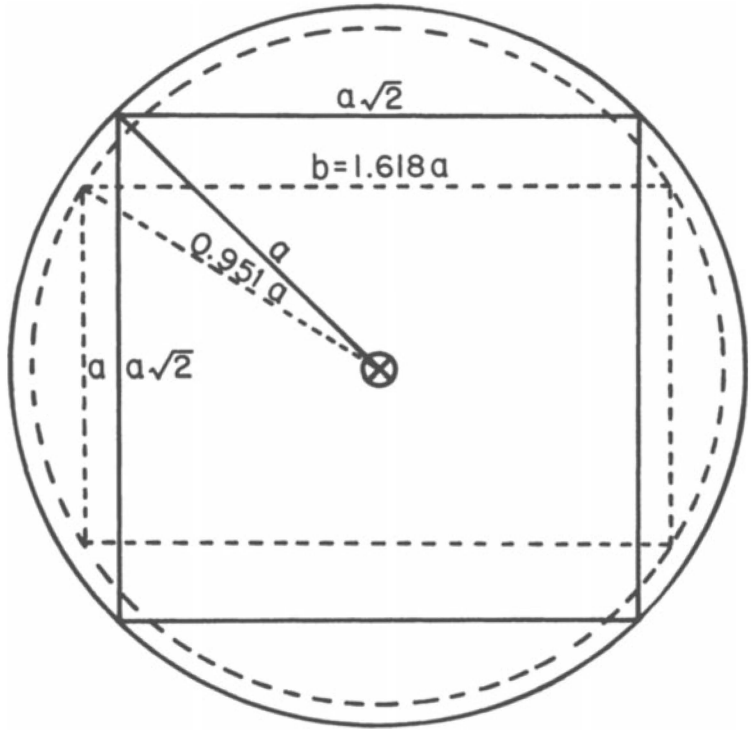

Figure 10. The metrical nature of the icosahedron (broken lines) as compared to that of the cubo-octahedron (solid lines). If a is the nearest vertex-to-vertex distance of each polyhedron, then the side of each square in Fig. 9c is $a \cdot \sqrt{2}$ (here, solid lines), and the rectangles in Fig. 9d have the sides a and b = 1.618 a (here, broken lines). It is seen that the icosahedron has a shorter center-to-vertex distance than the cubo-octahedron.

The cubo-octahedron (Fig. 9b) is brought into view through translation of the origin of the cube shown in Fig. 9a by one-half of the length of the cube edge along any one of the three axes or one-half of the body diagonal. It is seen (Fig. 9c) that the vertices of the cubo-octahedron are located at the corners of three intersecting, mutually perpendicular squares. If the edge length of the cubo-octahedron (bond distance) is a, then the side of each square is $a \cdot \sqrt{2}$. Replacement of each square by a rectangle that has the sides a and b = 1.618 a results in the configuration shown in Fig. 9d. It is called the icosahedron since it is bounded by twenty equilateral triangles.

Each corner of this polyhedron is connected with five other corners that form a plane pentagon. Each pentagon has the side a, and the distance between each corner and the next nearest corner is 1.618 a; that is, equal to the long side of the rectangle. There are, accordingly, many different orientations in which the set of three mutually perpendicular rectangles can be fitted into the upper part of Fig. 9d.

The icosahedron has 15 twofold axes (30 edges), 10 threefold axes (20 triangles), and 6 fivefold axes (12 vertices) as well as 15 planes of symmetry and other elements of the second kind.

The conversion of a cubo-octahedron, which has 24 nearest-neighbor distances (or edges) of length a, into an icosahedron of 30 nearest-neighbor distances of the same edge length a (replacement of the squares of side $a \cdot \sqrt{2}$ by rectangles of sides a and 1.618 a, Figs. 9c,d) results in a shortening of the center-to-vertex distance of 4.9 per cent and a corresponding decrease in volume of slightly more than 7 per cent, see Fig. 10. Accordingly, with twelve contiguous spheres of equal size at the vertices, the central sphere of the icosahedron has to be nearly 10 per cent smaller in radius.

From Fig. 9d it becomes immediately apparent that the icosahedron can be described also as a pentagonal antiprism, which has two atoms at the extended poles. It thus provides a condition favorable for the formation of tetrahedral interstices, which, in turn, result in a minimum of interstitial space. In fact, each icosahedron may be regarded as consisting of twenty contiguous and slightly deformed tetrahedra that have one vertex in common at the icosahedron center.

The icosahedron (pentagonal antiprism) is much more frequently observed than is the pentagonal prism (with two atoms at the extended poles), which gives rise to octahedral interstices, one around each center of a square prism face. The pentagonal prism corresponds to a radius ratio of nearly unity.

Of the three coordination shells of ligancy 12 discussed here, surrounding a central sphere which may become 10 per cent smaller, the icosahedron is the smallest (see Fig. 10) and hence corresponds to lower energy or higher stability.

To my knowledge a cubo-octahedron has not yet been observed in a true intermetallic compound; however, it is not uncommon in carbides, silicides, and interstitial compounds.

Irregular Coordination Shells of Ligancy 11, 13, and 14

Of the large variety of irregular coordination shells that exist, the three types described below occur most frequently in the giant cells: (1) A shell of ligancy 11 is formed by replacing the pentagon of an icosahedron with a tetragon. (2) Polyhedra of ligancy 13 are created through the widening of part of an icosahedron, and addition of a thirteenth ligand, that can penetrate the opening. (3) Ligancy 14 is produced through penetration of two of the approximately square prism faces of a pentagonal prism (occupied poles) by two atoms.

Interpenetrating and Contiguous Polyhedra

In a space-filling structure, the atoms at the vertices of any polyhedron are, in turn, surrounded by coordination shells that penetrate each other and the central one, and the various kinds of interpenetrating polyhedra are often incommensurate. This, as well as other factors that will be discussed later, leads to distortions, which sometimes become considerable. Therefore, throughout the discussions presented later, it should be understood that such terms as Friauf polyhedron, μ-phase polyhedron, icosahedron, etc., do not necessarily refer to the regular configurations in which each triangle is equilateral.

Because of interpenetration it is difficult to show by means of a model all existing polyhedra simultaneously. The figures shown in the following sections exhibit only the contiguous polyhedron; that is, those that share faces, edges, or corners but do not interpenetrate. In each such figure, each corner of a facet then represents the center of another coordination shell that has to be described in the text or shown in a separate model.

One of the most striking examples of interpenetrating polyhedra is found in the μ phase. In the close-packed layer of hexagonal bi-antiprisms shown in Fig. 6, each corner of a large hexagon represents the center of a μ-phase polyhedron, and thus, the layer shown in Fig. 4 represents exactly the same atomic arrangement as the one shown in Fig. 6. In fact, each hexagon that

can be made out in the horizontal plane in Fig. 4 belongs to a bi-antiprism, and the one shown at the rear, left-hand corner can be imagined as having been pulled out of that layer.

THE CRYSTAL STRUCTURES OF β Mg_2Al_3 AND $NaCd_2$

The structures of these two compounds are partially disordered but presumably in slightly different ways, as indicated by the difference between the two stoichiometric ratios. The fundamental structural features are the same, however. For βMg_2Al_3 the details of the disorder have been worked out,[9] but for $NaCd_2$ they are still uncertain.[15] $NaCd_2$ reacts with oxygen or moisture and gradually decomposes during X-ray examination. It is difficult, therefore, to obtain X-ray data of a quality that will suffice for the determination of all the structural details. Therefore, only βMg_2Al_3 is discussed below; the idealized ordered model is described first, and then some details of the disorder are given. The accurate length of the cube edge is $a_o = 28.239$Å for βMg_2Al_3 and $a_o = 30.56$Å for $NaCd_2$; the space group is in both cases $F_d3m(O_h^7)$.

The basic building block of the structure consists of five Friauf polyhedra that are arranged about an approximate fivefold axis of symmetry, as shown in Fig. 11. The five polyhedra are, in the crystallographic sense, of three different kinds (F1, F2, and F3). The group of polyhedra lies on a plane of symmetry; therefore, the left half of each figure is a mirror image of the right half. The dihedral angles of a tetrahedron are 70°32' and hence correspond to nearly one-fifth of a complete rotation. The aggregate (Fig. 11) consists of 47 atoms and is called the VF polyhedron. Each atom out from the center of a hexagon is not indicated for reasons explained earlier; see also Fig. 1.

Six VF polyhedra are arranged about the vertices of an octahedron in such a way as to produce four additional Friauf polyhedra, F4, located at the vertices of a regular tetrahedron and sharing hexagons with polyhedra F1. F4 is dark and only one is seen in Fig. 12. The resulting complex consists of 234 atoms and comprises 34 Friauf polyhedra. It has symmetry T_d (Fig. 12), and hence, each two diametrically opposed VF polyhedra are turned 90° with respect to one another. The twelve outer Friauf polyhedra are of the type F3.

A second such T_d complex is meshed with the first one, as shown in Fig. 13. These two complexes share hexagonal faces of the F2 polyhedra and are related to one another by a diamond glide. Three more T_d complexes can be added in a similar fashion. Each T_d complex is accordingly connected with four others that are

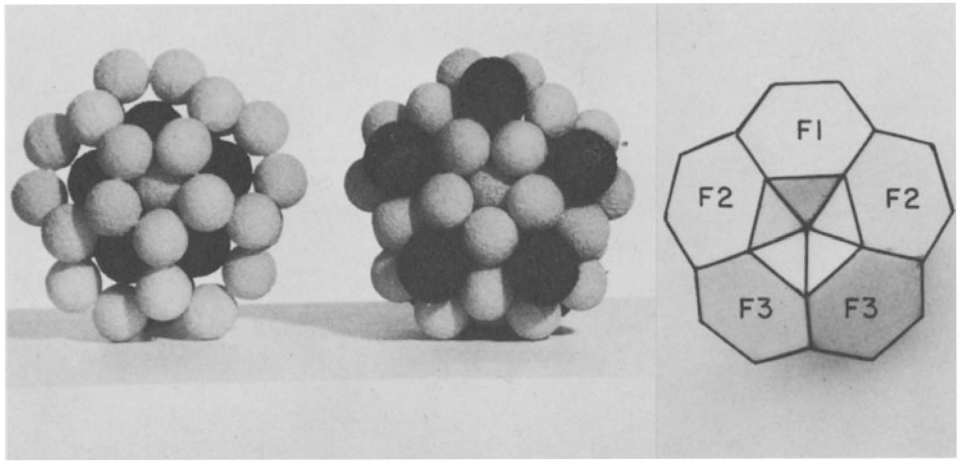

a b c

Figure 11. (a) Five contiguous truncated tetrahedra about a fivefold axis of symmetry. (b) The VF polyhedron. (c) A formal representation of the VF polyhedron. The atoms out from the centers of the hexagons are not indicated.

arranged about the vertices of a regular tetrahedron (Figs. 14 and 15). The atom out from the center of each dark hexagon of an F4 polyhedron is shared between three truncated tetrahedra, each one belonging to a Friauf polyhedron F3 of different T_d complex. A similar kind of vertex sharing is also observed in $\gamma Mg_{17}Al_{12}$,[16] and $\epsilon Mg_{23}Al_{30}$;[17] refer also to Fig. 25.

Continued stacking of T_d complexes leads to an infinite three-dimensional network (Fig. 16) in which each T_d complex of 234 atoms shares atoms with four others so as to reduce the average number of atoms per T_d complex to 144. The cubic unit of structure contains eight T_d complexes; they account for 1152 atoms. Eight more atoms (magnesium) have to be added, each of them at the center of a Friauf polyhedron F5 that cannot be brought into view with the opaque models used here. Each F5 polyhedron shares edges with twelve F3 polyhedra (that is, six VF polyhedra) and lies at the center of the sphere shown in Fig. 17. There are eight such spheres in the cubic unit; each one is penetrated by four others

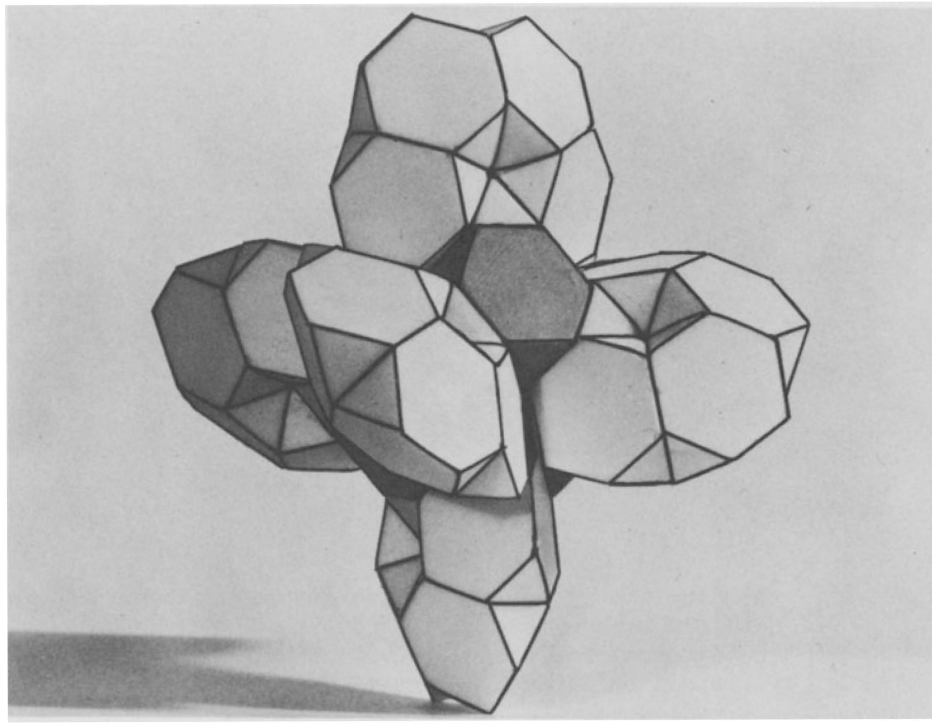

Figure 12. The complex of 234 atoms formed by six VF polyhedra that are arranged around the vertices of an octahedron of T_d symmetry. In the disordered model six of the twelve outermost Friauf polyhedra are distorted.

of the same kind. With the addition of 32 more atoms (aluminum) out from the centers of the triangles of eight such F5 polyhedra, the entire complement of 1192 atoms in the ordered structure is accounted for.

The unit of structure contains 280 Friauf polyhedra (L16), 96 μ-phase polyhedra (L15), 64 hexagonal antiprisms, each with two atoms at the extended poles (L14), 128 coordination shells of ligancy 13, and 624 icosahedra (L12). Each magnesium atom may be assumed to have ligancy 14, 15, or 16, and each aluminum atom, which is smaller (radius ratio Mg/Al $\sim$ 1.14), ligancy 12.

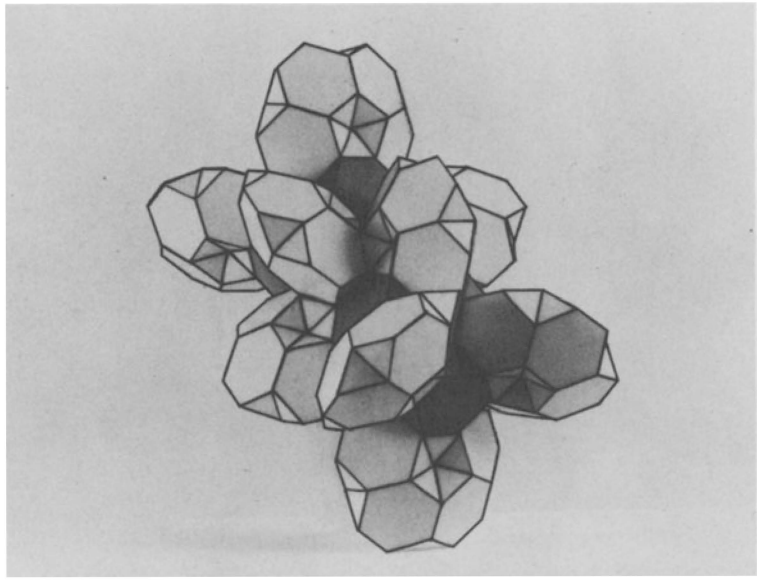

Figure 13. A second complex of 234 atoms inserted into the one shown in Fig. 12. The two complexes are related to each other by a diamond glide.

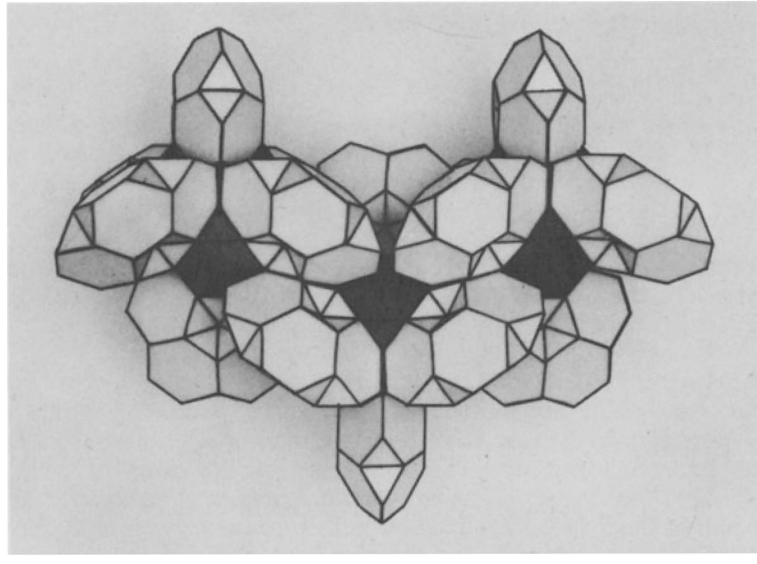

Figure 14. Three complexes of 234 atoms each forming part of the aggregate shown in Fig. 15.

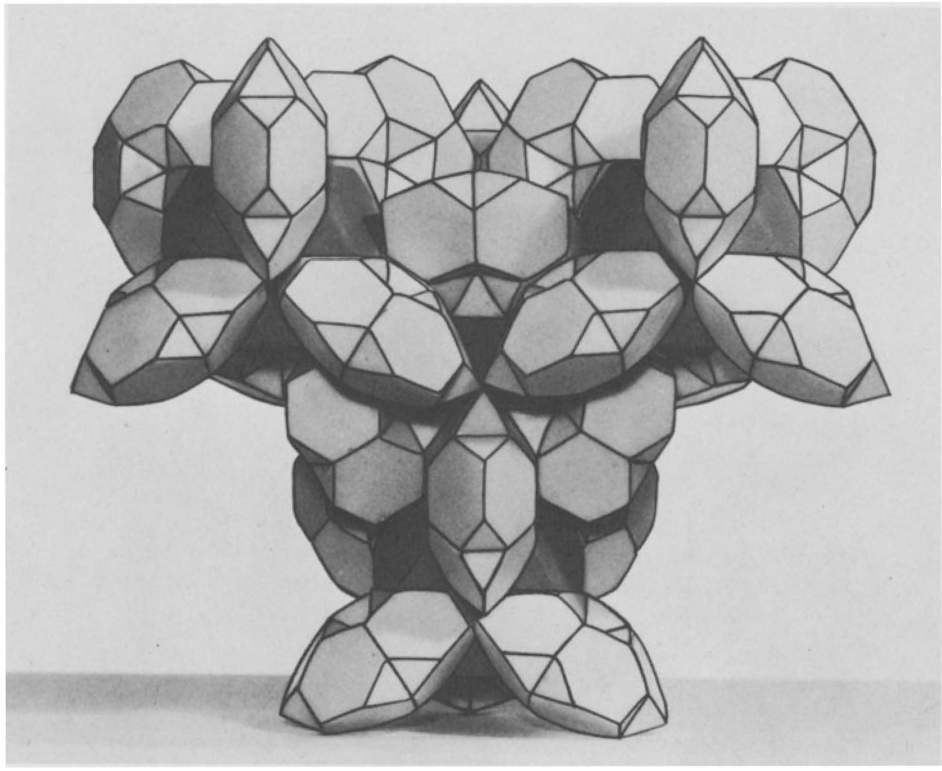

Figure 15. Four complexes of 234 atoms each arranged about one such complex. The four complexes are at the vertices of a regular tetrahedron.

Some of the coordination shells of ligancy 13 may enclose magnesium, and others aluminum. In this idealized ordered model the 1192 atoms occupy 17 different sets of equivalent positions.

The disordered model is obtained by replacing every other F5 polyhedron and the four associated aluminum atoms ($\frac{1}{8} \times 32$) with a centered pentagonal prism that has two atoms at the poles and two atoms out from the centers of two prism faces (complex of 15 atoms). In order that the observed space-group symmetry be retained, it has to be assumed that this 15-atom complex occurs in six orientations, and that there is a random interchange of the set of four F5 polyhedra and the set of four 15-atom complexes in the individual unit cells. The details of the disordered arrangement cannot be shown by

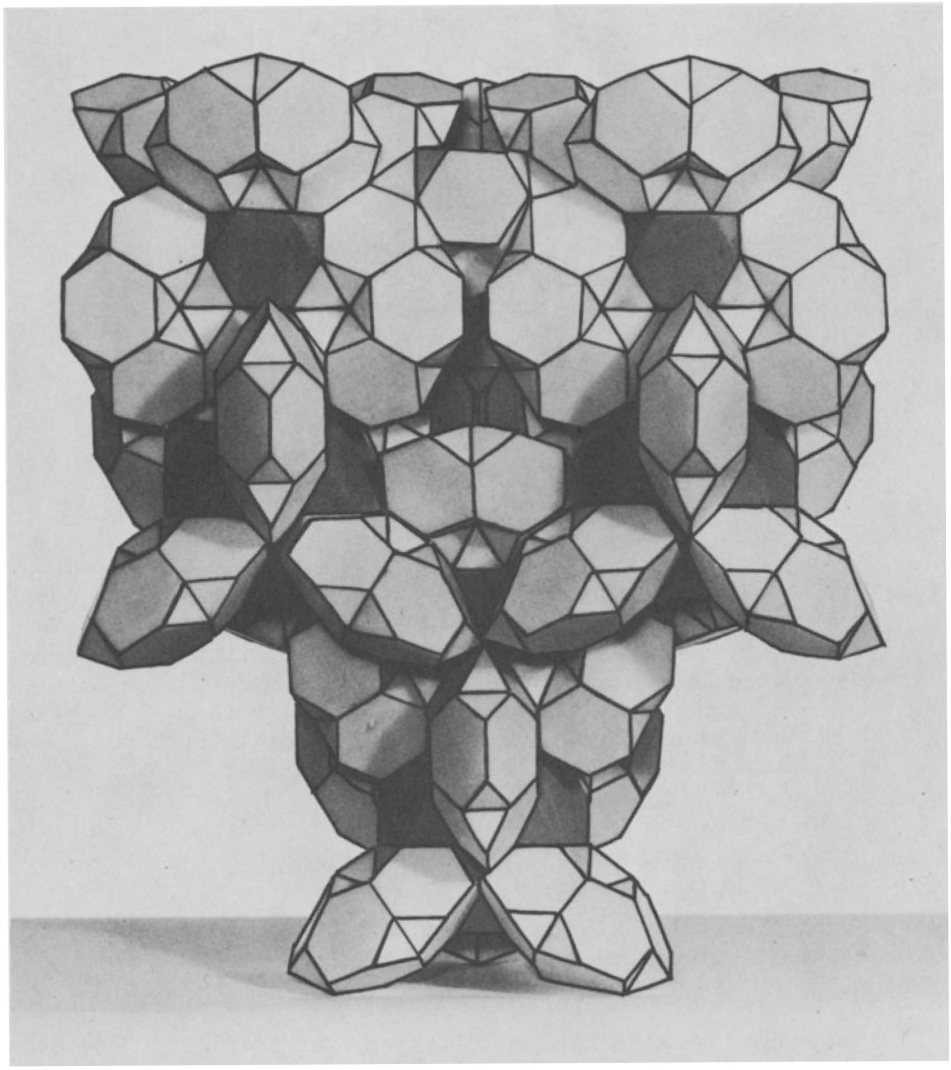

Figure 16. Continued stacking of the 234-atom complexes leads to the configuration shown above. The spherical arrangement of VF polyhedra shown in Fig. 17 can be recognized here. Its center is located about two-thirds up the vertical center line of this figure.

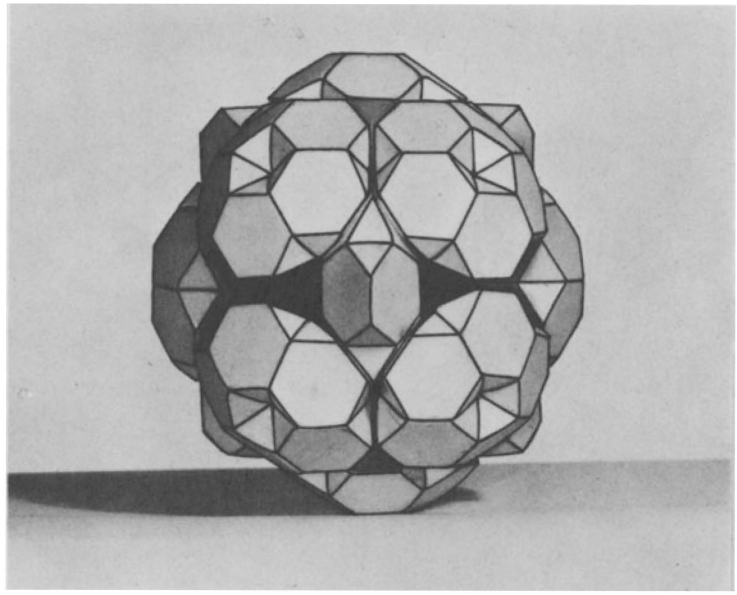

Figure 17. Twelve VF polyhedra (4 × 3) form a sphere around each one of the eight points $00\frac{1}{2}$, etc. Six additional VF polyhedra are arranged about the vertices of a second kind of T_d octahedron which can be made out on this figure. At the center of this sphere is a fifth kind of Friauf polyhedron, called F5, which is shared between these six VF polyhedra.

means of models of the kind presented here, but packing maps[18] are extremely well suited for this purpose as can be seen in the original paper.[9]

To account for this kind of disorder, the complex of 234 atoms (T_d complex) shown in Fig. 12 has now to be modified. Of any two diametrically opposed VF polyhedra in this complex, one remains unchanged, while the other contains, instead of two F3 polyhedra, two modified Friauf polyhedra.

In the three-dimensional network of the modified T_d complexes each second sphere of the kind shown in Fig. 17 will then have a 15-atom complex at its center instead of the F5 polyhedron with the associated four aluminum atoms (21-atom complex). Since there are four spheres of each kind per unit of structure, the total number of

atoms is 1192 - 4 (21 - 15) = 1168. The occurrence of the 15-atom complexes in six orientations results in the displacement of certain other atoms in the structure for part of the time.

The atoms of the disordered model occupy 23 different sets of equivalent positions. In an ordered structure, the number of different polyhedra is equal to the number of point sets; but here, the number of different polyhedra (in the crystallographic sense) is increased to 41. The disordered atomic arrangement corresponds to 252 Friauf polyhedra, 24 μ-phase polyhedra, 48 hexagonal antiprisms (plus two atoms at the extended poles), 672 icosahedra, and 172 more-or-less irregular coordination shells of ligancy 10 to 16, forty-eight of which are modified Friauf polyhedra. The disorder, accordingly, results in a gain of 48 icosahedra per unit of structure.

Some Notes on the Derivation of this Structure

As is seen, the idealized ordered model has been completely accounted for with the use of only five crystallographically different Friauf polyhedra (except for the 32 atoms that had to be added out from the triangles of the eight F5 polyhedra; the eight extra magnesium atoms added belong to F5), whereas the (ordered) structural unit comprises seventeen crystallographically different kinds of polyhedra. The Friauf polyhedra dominate the structure, although they are by far outnumbered by the other kinds of coordination shells, especially by icosahedra; this is because the truncated tetrahedra do not penetrate one another.

In any structure so far known to incorporate Friauf polyhedra, the truncated tetrahedra are contiguous; thus far they have never been observed to penetrate each other. The Friauf-polyhedra framework, therefore, represents the most favorable starting point in the search for a trial structure in which it is anticipated.

This observation has been of extreme importance in the derivation of this structure as well as that of Cu_4Cd_3[6] and others,[19,20] in which packing maps[18] had to be used. Probably it would have been possible to deduce the trial structure by starting out with icosahedra. A few of them placed at appropriate points on the packing map[18] would have suggested the existence of Friauf polyhedra, and from here on there would not have been too much reasonable latitude for the positioning of the remaining atoms. This approach would have been considerably more tedious and difficult, however.

THE CRYSTAL STRUCTURE OF Cu_4Cd_3

Although the unit of structure of this compound contains somewhat fewer atoms than that of βMg_2Al_3 (and $NaCd_2$), 1124 as compared

to 1168 per unit cube, it was considerably more difficult to determine. The reason for this is the lower symmetry and a resulting significant increase in the number of structural parameters. The space group is $F\bar{4}3m(T_d^2)$ and the more accurate length of the cube edge is $a_o = 25.871$Å. In fact, this structure comprises two different substructures that penetrate one another, and each one is of considerable complexity. Each substructure represents a diamond arrangement, in one case of Friauf polyhedra, in the other case of icosahedra. The structure lacks a center of symmetry, and hence calculations of Fourier syntheses are meaningless unless the trial models of both substructures are nearly correct and are used simultaneously as a basis for the phase-angle determinations. Again, the structure was solved exclusively with the use of a packing map.

The metallic radius observed for cadmium in intermetallic compounds is almost identical to that observed for magnesium, whereas copper atoms are somewhat smaller than aluminum atoms. The difference in size is appropriate for the formation of Friauf polyhedra, each with cadmium at the center and copper at the vertices of the truncated tetrahedron.

The diamondlike arrangement of Friauf polyhedra consists of the three types of complexes shown in Figs. 18a, b, and c. The octahedron of T_d symmetry, Fig. 18a, comprises ten Friauf polyhedra (4 F1 + 6 F2). The tetrahedral arrangement shown in Fig. 18c consists of five Friauf polyhedra (F5 + 4 F6), and the four dark polyhedra in Fig. 18b are F3 + 3 F4. The cubic unit contains four octahedra (Fig. 18a) that are arranged about the points $\frac{1}{2},\frac{1}{2},\frac{1}{2}$; $\frac{1}{2}00$; $0\frac{1}{2}0$; $00\frac{1}{2}$ (point set 4b in $F\bar{4}3m$) and four tetrahedra (Fig. 18c) that are at the points $\frac{1}{4},\frac{1}{4},\frac{1}{4}$, etc. (point set 4c). The layer of the dark Friauf polyhedra serves as a link between the octahedra and the tetrahedra. The infinite, three-dimensional framework of Friauf polyhedra thus formed is shown in Fig. 19. It is seen that the tetrahedra, the dark layers, and the octahedra alternate in a zigzag fashion.

The diamondlike arrangement of icosahedra may be described in terms of two kinds of complexes. One of them is shown in Fig. 20. It is seen (Fig. 20a) that five icosahedra, sharing vertices, are arranged about an approximate fivefold axis of symmetry, thus enclosing a pentagonal prism; each shared vertex represents also the center of a pentagonal prism. A set of six such fivefold rings is arranged at the vertices of an octahedron of T_d symmetry. All six rings interpenetrate and share icosahedra in such a way that the aggregate (Fig. 20c) consists of fourteen icosahedra that enclose six pentagonal prisms of the kind shown in Fig. 20a. Figure 20b shows two such fivefold rings interpenetrating at right angles. It is now seen that the pentagonal prism (in Fig. 20a) is shared by two icosahedra, one above and the other below the plane of the paper.

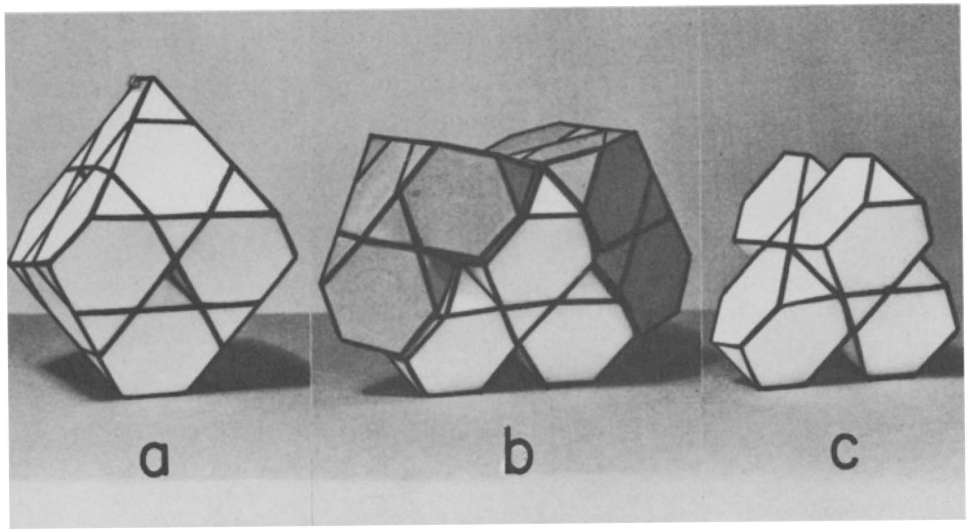

Figure 18. The three types of atomic groupings that form the infinite, three-dimensional framework of Friauf polyhedra shown in Fig. 19. (a) A complex of ten Friauf polyhedra forming an octahedron of T_d symmetry. (b) The dark Friauf polyhedra attached to the complex shown in (c) serve as a link between (a) and (c). (c) Five Friauf polyhedra arranged to form a tetrahedron.

The two icosahedra have one vertex in common at the center of the pentagonal prism, and each icosahedron center is at an extended pole of that prism. Each additional vertex that is shared between two icosahedra represents the center of a pentagonal prism (which has two atoms at its extended poles), as can be made out on the figures. Accordingly, thirty-six more pentagonal prisms are created. In twelve of these prisms, two prism faces are deformed in such a way that two more atoms are added as ligands (to provide ligancy 14).

Accordingly, the aggregate shown in Fig. 20c represents fourteen icosahedra, thirty pentagonal prisms, each one with two atoms at the poles (ligancy 12), and twelve pentagonal prisms, each of which has two more atoms penetrating two prism faces (ligancy 14).

The second icosahedral complex is shown in Fig. 21c. It consists of a set of six pairs of interpenetrating icosahedra. The center of each icosahedron of such a pair represents a vertex of the

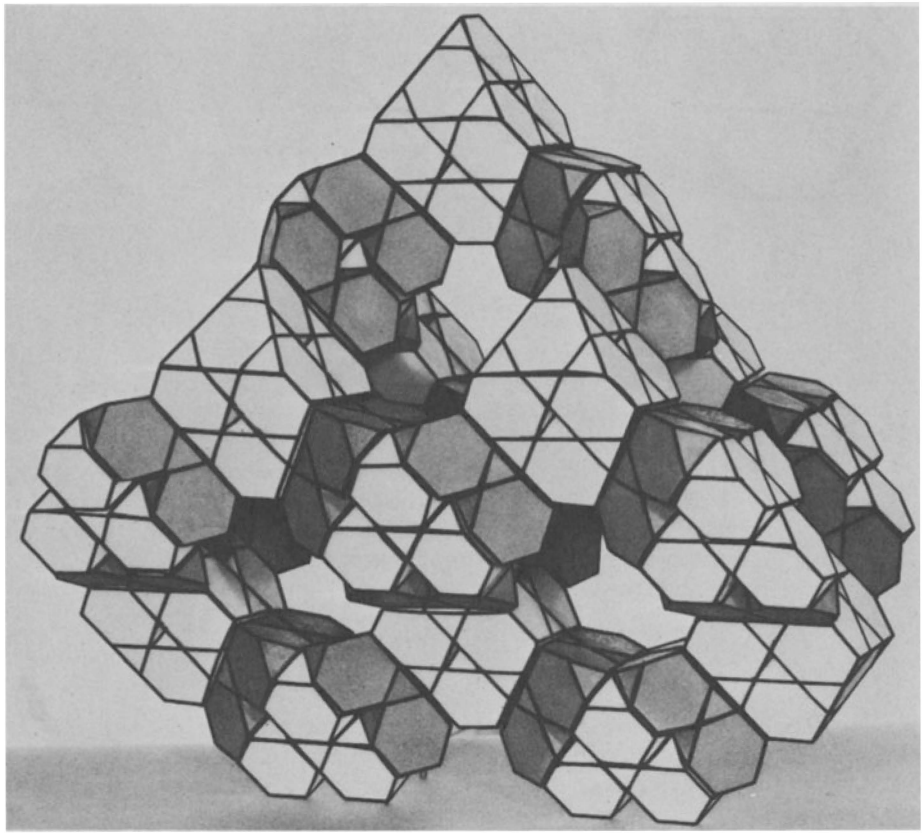

Figure 19. The three complexes shown in Figs. 18a,b,c are arranged in a zigzag fashion to form an infinite, three-dimensional framework, part of which is shown here.

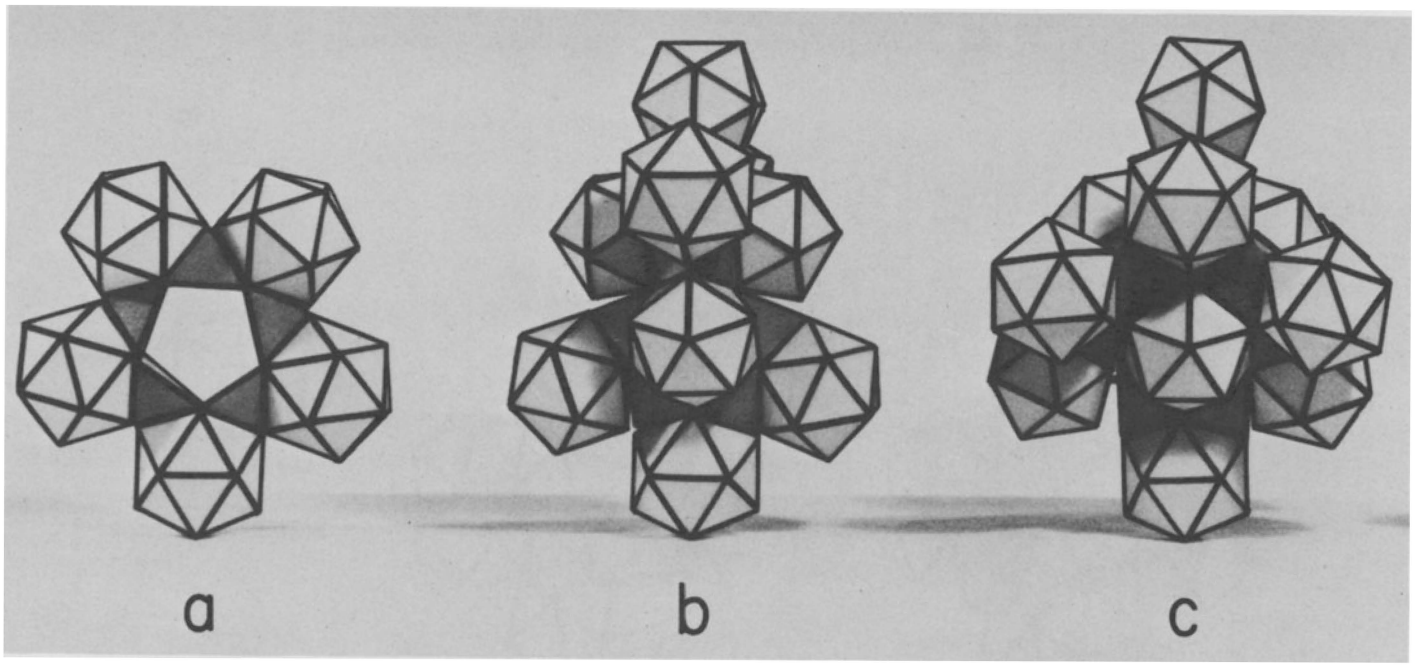

Figure 20. (a) Five icosahedra, sharing corners, arranged about an approximate fivefold axis of symmetry. (b) Two such fivefold rings interpenetrate at right angles. (c) Six interpenetrating fivefold rings form a complex of fourteen icosahedra and forty-two centered pentagonal prisms.

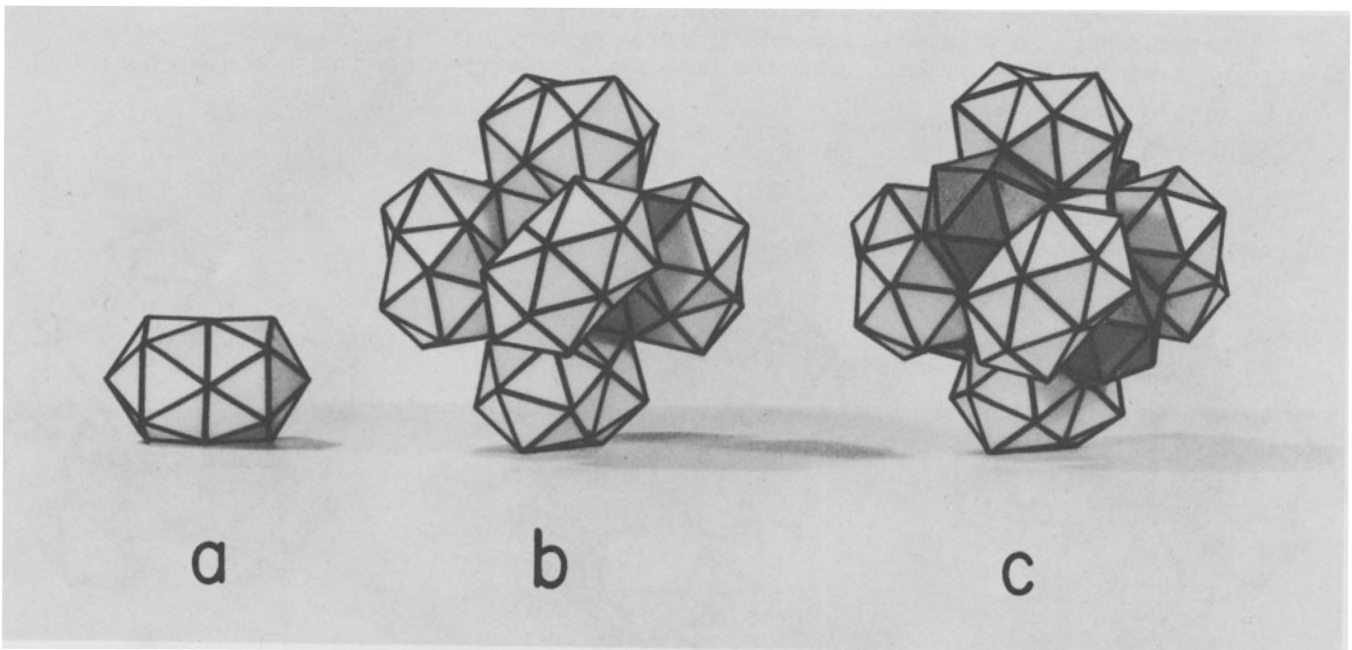

Figure 21. (a) Two interpenetrating icosahedra, referred to as a pair. The center of each of these icosahedra represents a vertex of the other. (b) A set of six such pairs arranged about the vertex of an octahedron of T_d symmetry. (c) Four more icosahedra, the dark ones, have been added to form a complex of sixteen icosahedra and eighteen pentagonal prisms.

other, as can be made out in Fig. 21a. The center of each pair (that is, the center of each shared pentagon) is at the vertex of an octahedron of T_d symmetry; accordingly, each one of two diametrically opposed pairs has its fivefold axis (long axis) at a right angle to that of the other (Fig. 21b). Four more icosahedra have to be inserted into this complex. Their centers are at the vertices of a regular tetrahedron, and each of these icosahedra shares six triangles with three "icosahedron pairs" that surround it, as is shown in Fig. 21c. The four icosahedra are the dark ones in Fig. 21c. Each vertex that is shared between two icosahedron pairs is, again, the center of a pentagonal prism, which has two atoms at the extended poles and two additional atoms that penetrate two of the prism faces (ligancy 14). Several of the pentagonal prisms can be made out in Fig. 21b, especially at the upper left.

The aggregate shown in Fig. 21c thus represents sixteen icosahedra and eighteen pentagonal prisms.

The cubic unit contains four aggregates of the kind shown in Fig. 20c and four of the kind shown in Fig. 21c. The former aggregates are arranged about the points $\frac{5}{4},\frac{3}{4},\frac{5}{4}$, etc. (point set 4d) and the latter about the points 0,0,0, etc. (point set 4a). Both types of aggregates are connected with one another by shared vertices in such a way that twelve more pentagonal prisms (plus two atoms at the poles, ligancy 12) are formed between each two complexes. The two types of aggregates (Figs. 20c and 21c) thus form the infinite, three-dimensional framework shown in Fig. 22. The dark icosahedra shown in Fig. 21c have been omitted in this large model, since they are difficult to insert.

The framework of icosahedra (Fig. 22) fits into the cavities of the Friauf-polyhedra framework shown in Fig. 19. Both frameworks share vertices in such a way that additional coordination shells are produced, most of them icosahedra, that penetrate the Friauf polyhedra as well as the icosahedra described above.

The unit cube of structure contains 124 Friauf polyhedra (L16); 144 μ-phase polyhedra (L15); 120 centered pentagonal prisms, each one with two atoms at the extended poles, and two additional atoms out from the centers of two prism faces (L14); 168 centered pentagonal prisms, each one with two atoms at the extended poles (L12); 568 centered icosahedra (L12).

In terms of the unit-cell content the composition can be written $Cu_{640}Cd_{484}$, and the 1124 atoms are distributed among 29 sets of equivalent positions.

There appears to be a correlation between the two interpenetrating framework structures and the structures of the two phases that form the metastable eutectic mixture that reacts to give this

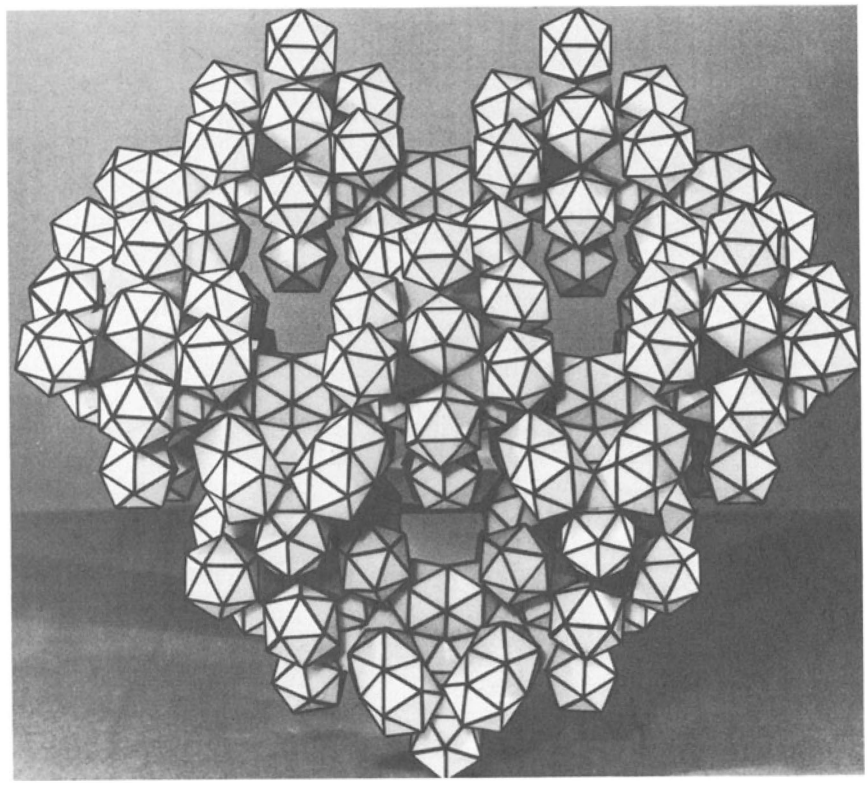

Figure 22. The two complexes of icosahedra shown in Figs. 20 and 21 share vertices with one another to form the diamondlike, infinite, three-dimensional framework shown here. This framework fits into the cavities formed by the Friauf polyhedra framework shown in Fig. 19.

phase (see introduction). One of these is $CdCu_2$ with the C36 type of structure, the other is Cd_8Cu_5 with the $D8_2$ type of structure (γ-brass), which is known to be essentially icosahedral. Parts of these two structures are retained in the two frameworks. The zigzag chain of Friauf polyhedra shown in Fig. 19 corresponds to a mixture of the C14, C15, and C36 ($MgZn_2$, $MgCu_2$, $MgNi_2$) types of structure; refer also to Fig. 24.

Some Notes on the Derivation of this Structure

In this case, we had to resort to six crystallographically different Friauf polyhedra and five different icosahedra to describe the model, whereas in the case of βMg_2Al_3 only five different Friauf polyhedra were needed. This implies that the derivation of the trial structure of Cu_4Cd_3 by means of packing maps involves the fitting of more than twice as many different polyhedra as does the derivation of the idealized ordered model of βMg_2Al_3.

The Friauf polyhedra framework shown in Fig. 19 was relatively easy to derive. A perfect geometrical fit of the set of six polyhedra (F1 to F6; see original paper[6] and Fig. 23) on the packing map enabled me to place reliance upon this part (about 50%) of the structure. From here on I had to resort to a few other rules that I formulated on the basis of observation of an extensive number of other structures that incorporate Friauf polyhedra.[21] Two of these rules are: (1) In infinite, three-dimensional frameworks of Friauf polyhedra, each hexagon of a truncated tetrahedron, not shared by another truncated tetrahedron, is usually shared by a hexagonal antiprism that has two atoms at the extended poles (L14) or by a μ-phase polyhedron (L15). These two polyhedra often terminate groupings of Friauf polyhedra; see also Figs. 7 and 8. (2) In each case where Friauf polyhedra form rows, layers, or three-dimensional frameworks, each truncated tetrahedron is penetrated most often by twelve icosahedra and sometimes by nine or more icosahedra and three or less coordination shells of ligancy 13 or 14.

In accordance with these principles, I explored the possibility of constructing an icosahedron around each vertex of a truncated tetrahedron that was laid out on the packing map. The orientation of each icosahedron is determined by the Friauf polyhedron. There were, furthermore, only two kinds of hexagons of truncated tetrahedra (F2 and F4) that were not shared with other truncated tetrahedra, and these then became shared with μ-phase polyhedra. After addition of a few more atoms, the structural motif represented by the five icosahedra about the fivefold axis of symmetry unfolded; see Fig. 20.

A packing map of Cu_4Cd_3 is shown in Fig. 23. Here are emphasized by shaded areas only those polyhedra that create the structural

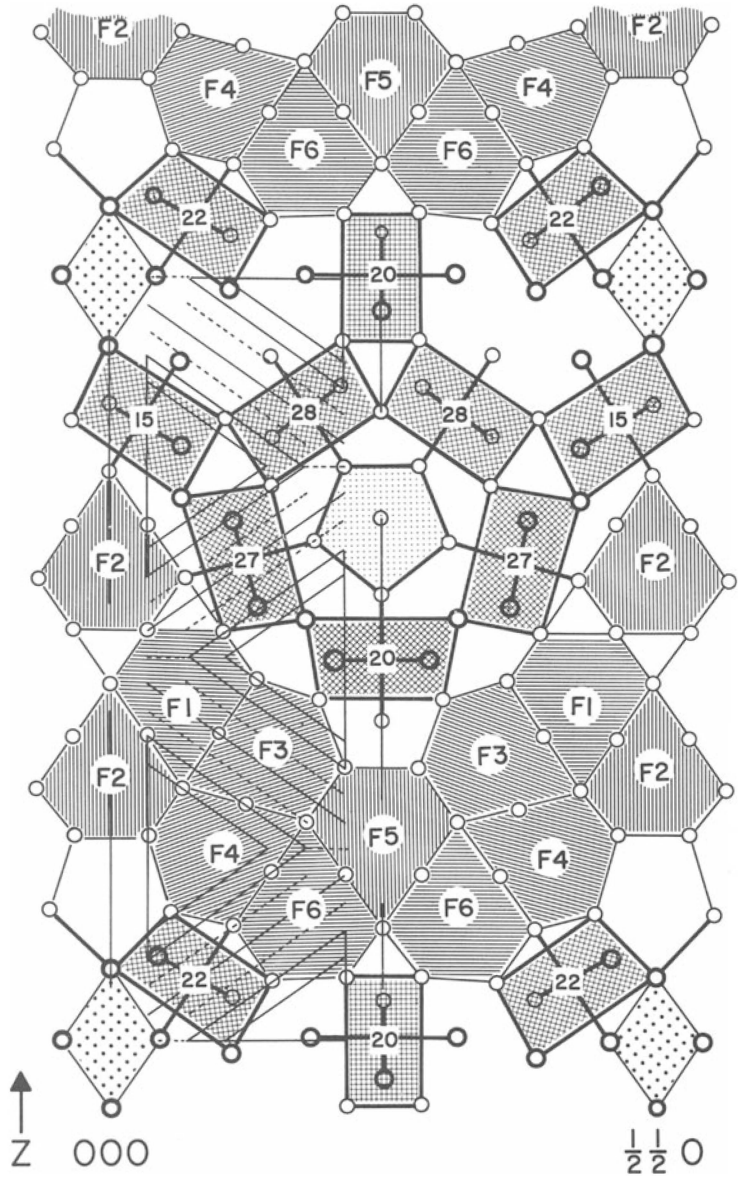

Figure 23. The packing map of the structure of Cu_4Cd_3. Here are emphasized by shaded areas the polygonal sections of only those polyhedra that produce the structural motifs shown in Figs. 18 to 22. F1 to F6 represent sectioned Friauf polyhedra and the numbers 15, 20, 22 ··· are inside sectioned icosahedra. It is seen that the rectangles (compare with Fig. 9d) are slightly deformed.

motifs discussed in the preceding section. The rectangles marked 20, 27, and 28 are the sectioned icosahedra of the complex shown in Fig. 20, the rectangles marked 15 and 22 form the complex shown in Fig. 21, and F1 to F6 represent the framework shown in Fig. 19. The interpenetrating icosahedra around the vertices of the truncated tetrahedra that were used for the derivation, as discussed above, are not emphasized here, but they can be traced out by the reader. The μ-phase polyhedron that shares a hexagon with F2 can be traced out also. In fact, every structural detail of Cu_4Cd_3 can be read from this figure by a trained user of packing maps.

COMMON STRUCTURAL FEATURES IN INTERMETALLIC COMPOUNDS CONTAINING FRIAUF POLYHEDRA

The different types of structures that contain Friauf polyhedra are: (1) $MgCu_2$ and $MgZn_2$ [C15 and C14 types, Friauf phases[10,11]]; (2) $MgNi_2$ [C36 type, Laves phase[12]]; (3) MgCuAl [mixture of the two Friauf phases and the Laves phase, Komura[22]]; (4) W_6Fe_7 [μ phases[13]]; (5a) P(Mo-Ni-Cr) [P phases[14]]; (5b) δ(Mo-Ni) [δ phases, closely related to the P phase[23]]; (6a) $Mg_3Cr_2Al_{18}$ [E phase[19]]; (6b) $ZrZn_{22}$ and other AB_{22} compounds [closely related to (6a)[20,29]]; (6c) αVAl_{10} [closely related to (6a)[24,32]]; (7a) αMn [χ phases[25,26]]; (7b) $\gamma Mg_{17}Al_{12}$ [closely related to (7a)[16]]; (8a) R(Mo-Co-Cr) [R phases[27]]; (8b) $\epsilon Mg_{23}Al_{30}$ [closely related to R phases[17]]; (9) $Mg_{32}(Zn,Al)_{49}$ [T phase[28]]; (10a) $NaCd_2$[15]; (10b) βMg_2Al_3 [closely related to (10a)9]; (11) Cu_4Cd_3.[6]

Figure 24 shows the basic simple modes in which truncated tetrahedra are connected with each other and with other kinds of coordination shells. Each of the structures referred to in (1), (2), and (3) above can be described in terms of layers of close-packed Friauf polyhedra (see also Fig. 2); they differ only in the way the layers are superimposed on one another.

In $MgCu_2$ each Friauf polyhedron of the second layers is turned 60° with respect to that of the first, as is shown in Fig. 24a (mode I), whereas in $MgZn_2$ the second Friauf polyhedron is a mirror image of the first one (mode II, Fig. 24b). In $MgNi_2$ both modes occur alternately in the hexagonal c direction. A variation in sequence of the two modes (I and II) leads to an ever-increasing length of the period (hexagonal c axis). Striking examples of this are the two known modifications of MgCuAl, one with c_0 = 21.05Å, the other with c_0 = 37.89Å.

The zigzag chain of the Friauf polyhedra framework of Cu_4Cd_3 (Fig. 19) exhibits the two modes in the sequence I-II-II-I.

Each hexagon of F2 and F4 in Cu_4Cd_3 that is not shared with another truncated tetrahedron is shared with a μ-phase polyhedron,

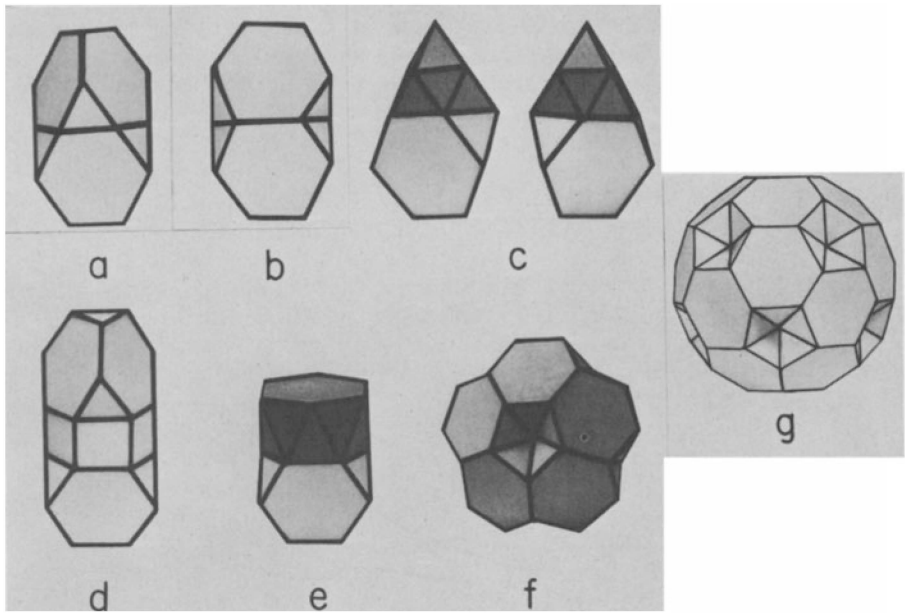

Figure 24. The basic, simple modes in which truncated tetrahedra are connected with each other and with other polyhedra: (a) Two Friauf polyhedra forming mode I; C15 type, βMg_2Al_3, and Cu_4Cd_3. (b) Two Friauf polyhedra in mode II; C14 type, βMg_2Al_3, and Cu_4Cd_3. (c) A Friauf polyhedron (light) and a μ-phase polyhedron (dark). Both figures represent the same mode III (see text); P phase, $Mg_{32}(Zn,Al)_{49}$, and Cu_4Cd_3. (d) Two Friauf polyhedra connected via a hexagonal prism. Two modes are possible but only this one (mode IV) has as yet been observed; $Mg_3Cr_2Al_{18}$, AB_{22}, and αVAl_{10}. (e) A Friauf polyhedron (light) and a hexagonal antiprism (dark) referred to as mode V; μ phase, P phase, and βMg_2Al_3. (f) Five Friauf polyhedra forming the VF polyhedron (mode VI); βMg_2Al_3 and $Mg_{32}(Zn,Al)_{49}$. (g) Twenty Friauf polyhedra forming a truncated icosahedron; $Mg_{32}(Zn,Al)_{49}$. Note that the C36 type and MgCuAl represent a mixture of the modes I and II.

as shown in Fig. 24c. The geometrical nature of the two polyhedra is such that there exists only one mode (mode III); rotation of the μ-phase polyhedron (dark) by 60° with respect to the Friauf polyhedron (light) results in a picture equivalent to that obtained by rotating the whole aggregate 180° so that its rear view can be seen. Both front and rear views are shown in Fig. 24c. This combination occurs also in the structures referred to in (5a,b), (8a,b), (9), and (10a,b) above.

The combination of Friauf polyhedra and hexagonal prisms (Fig. 24d) is extremely rare and occurs only in the structures (6a,b,c). It seems to eliminate the possibility that the atoms at the corners of the shared hexagons surround themselves with icosahedral coordination shells. The structures (6a,b,c) exhibit a relatively large number of square configurations and octahedral interstices.

Association between a truncated tetrahedron and a hexagonal antiprism (Fig. 24e) is observed in all cases except in (1), (2), (3), (6a,b,c), and Cu_4Cd_3 (11) above.

The VF aggregate (Fig. 24f) is represented not only by $NaCd_2$ and βMg_2Al_3 (10a,b) but also by $Mg_{32}(Zn,Al)_{49}$ (9). Here, each one of twenty truncated tetrahedra has its center at the vertex of a pentagonal dodecahedron. The resulting configuration is the truncated icosahedron shown in Fig. 24g. It is seen that here twelve interpenetrating VF aggregates are arranged about the vertices of an icosahedron. At the center of this complex is an icosahedron that is created by the triangles of the twenty contiguous truncated tetrahedra. This aggregate represents 113 atoms.

MISFIT OF POLYHEDRA

Manifestation of Disorder

The arrangements of Friauf polyhedra shown in Fig. 25 exhibit geometrical properties that deserve special attention. It is seen that in each of these the atom out from a certain hexagon (A atom), which normally is of the large kind, represents simultaneously the vertex of a truncated tetrahedron, at which a small atom (B atom) normally is expected. This vertex, accordingly, fills two disparate functions and therefore is called the bifunctional or hybrid vertex.[17,21] The coordination shell around this vertex is sometimes of the intermediate ligancy 14 (βMg_2Al_3, $\epsilon Mg_{23}Al_{30}$, and R phases) and sometimes of ligancy 13 ($\gamma Mg_{17}Al_{12}$ and X phases).

There are three different modes, in which hybrid vertices are created, as is shown in Fig. 25. If each truncated tetrahedron were regular and each of its 18 edges were of length a, then the dihedral angle between the hexagon and the equilateral triangle shown in

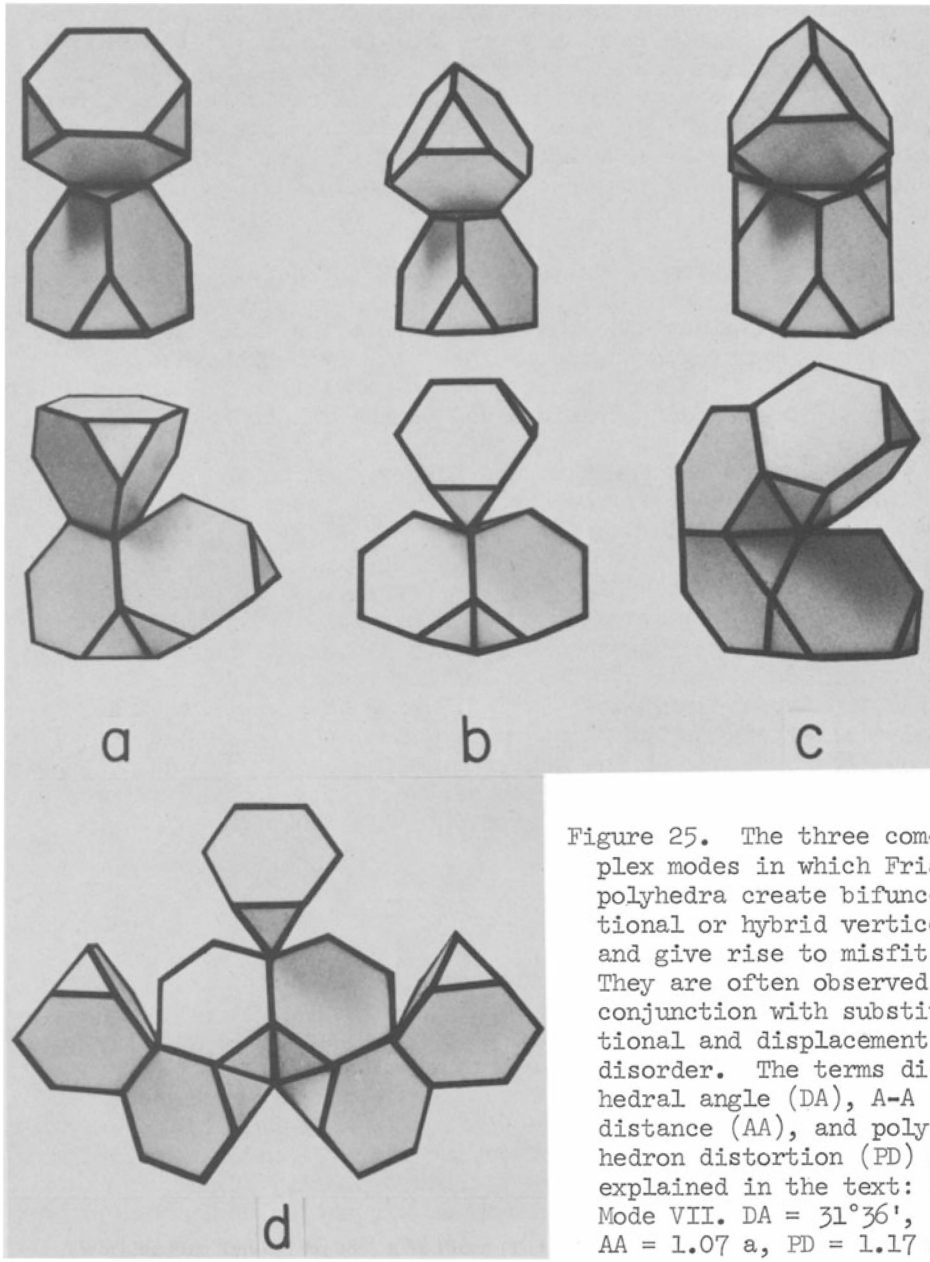

Figure 25. The three complex modes in which Friauf polyhedra create bifunctional or hybrid vertices and give rise to misfit. They are often observed in conjunction with substitutional and displacement disorder. The terms dihedral angle (DA), A-A distance (AA), and polyhedron distortion (PD) are explained in the text: (a) Mode VII. DA = 31°36', AA = 1.07 a, PD = 1.17 a; in $\gamma Mg_{17}Al_{12}$, χ phases, and βMg_2Al_3. (b) Mode VIII. DA = 35°16', AA = 1.12 a, PD = 1.22 a; in βMg_2Al_3 only. (c) Mode IX. DA = 38°56', AA = 1.17 a, PD = 1.29 a; in $\epsilon Mg_{23}Al_{30}$ and R phases. (d) Mixture of modes VII and VIII, as observed in βMg_2Al_3. The four Friauf polyhedra forming the arch belong to a VF polyhedron.

Fig. 25a (mode VII) would be 31°36', in Fig. 25b (mode VIII) 35°16', and in Fig. 25c (mode IX) 38°56'. In each case the hybrid vertex lies below the normal that passes through the center of the hexagon. In order that this vertex be equidistant from all six corners of the hexagon (with the dihedral angles unchanged) the equilateral triangle has to be converted into an isosceles triangle in which the two shanks are of length 1.17 a (mode VII), 1.22 a (mode VIII), or 1.29 a (mode IX), which involves a significant distortion. The distance between the hybrid vertex and the center of the adjacent Friauf polyhedron (A-A distance) is 1.07 a for mode VII, 1.12 a for mode VIII, and 1.17 a for mode IX, whereas the center-to-center distance between two truncated tetrahedra that share a hexagon [normal modes I and II (Fig. 24a,b)] is 1.23 a.

It is seen that at least one of the Friauf polyhedra must be significantly distorted, although all the truncated tetrahedra may be regular, as is the case in Fig. 25. The creation of the hybrid vertices, accordingly, is associated with a considerable degree of misfit. This feature, in addition to the bifunctional character, suggests that the hybrid vertices may favor substitutional and displacement disorder.

Mode VII is represented by $\gamma Mg_{17}Al_{12}$ in which slightly more than eight magnesium atoms (large) per structural unit can be replaced by aluminum atoms (small) to give $\gamma Mg_{13}Al_{16}$ (radius ratio Mg/Al $\sim$1.14). The aluminum-rich compound is metastable at room temperature and transforms on annealing at or below 370°C to $\epsilon Mg_{23}Al_{30}$,[17] which represents mode IX (Fig. 25c). It seems likely that the substitutional disorder, which must be associated with the large homogeneity range, is confined to the bifunctional vertices. There are 24 such vertices in the unit of structure, and the composition $Mg_{17}Al_{12}$ is the one that corresponds to the 100 per cent occupancy of these vertices by large atoms (magnesium).

The well-known χ phases[26] are isostructural with $\gamma Mg_{17}Al_{12}$ and the R phases,[27] which show a high degree of disorder, are nearly isostructural with $\epsilon Mg_{23}Al_{30}$.

In βMg_2Al_3 the two kinds of hybrid vertices shown in Figs. 25a and b occur simultaneously and affect the Friauf polyhedra called F3 and F5, as is shown in Fig. 25d. Here, the vertex of mode VIII was found to be displaced part of the time (see atom No. 19 in Fig. 11 of the original paper[9]). The Friauf polyhedron which is on top of the two contiguous polyhedra, as shown in Figs. 25b and d, is the one called F5 in βMg_2Al_3, and the partial disorder observed here is confined to this region of the structure, as has been pointed out earlier and also in the original paper.[9]

In view of the resulting misfit, the frequent occurrence of the hybrid vertices seems surprisingly high. As we have seen, the

hybrid vertices seem to be associated with large homogeneity ranges, substitutional disorder, or displacement disorder, with the possible exception of $\epsilon Mg_{23}Al_{30}$, which seems to have a narrow homogeneity range.[33]

INTERACTION BETWEEN Friauf POLYHEDRA AND ICOSAHEDRA

In almost each type of structure so far discussed, the Friauf polyhedra are by far outnumbered by icosahedra. This is caused by the fact that between ten and twelve vertices of each truncated tetrahedron are centers of icosahedral coordination shells. These penetrate the Friauf polyhedra in such a manner that in almost each case about one-half of their vertices are occupied by large atoms (A atoms) and the other half by small atoms (B atoms). Thus, the average effective size of the atoms at vertices of each icosahedron corresponds to a central atom that is approximately ten per cent smaller, the nominal radius ratio Mg/Al, corrected for the proper ligancies (L16 and L12, respectively), is about 1.14.

In the infinite, three-dimensional framework of Friauf polyhedra shown in Fig. 19, each corner of a facet represents an icosahedron center. The basic building block thus appears to be the icosahedron, and the Friauf-polyhedra framework may be regarded as describing the modes, in which the icosahedra are arranged with respect to one another.

The two kinds of interpenetrating polyhedra are not commensurate, that is, both cannot be regular simultaneously; either one or both of them have to be deformed. The nature of deformation depends upon the mode of interpenetration, which, in turn, depends upon the orientation of the Friauf polyhedra with respect to one another in the various types of structures.

Deformation provides flexibility with regard not only to the effective size but also to the effective shape of the atom at the center of a coordination shell. The degree of distortion of the one shell relative to the other probably depends upon the power of each species of atoms (say, A atoms and B atoms in Friauf structures) to enforce its coordination requirements. It seems possible, therefore, that the diversity of environment in the extremely complex structures results from the fact that the atoms have assumed positions relative to one another which are characteristic of their individual sizes, shapes, and bond-forming powers, whereas a simple structure may involve adjustment of one atom to another in such a way that only an average value of atomic properties finds expression.

POSSIBLE FACTORS DETERMINING STABILITY

A striking feature of the most common coordination shells observed here is the frequent occurrence of triangular faces; the Friauf polyhedron is bounded by 28 triangles, the μ-phase polyhedron by 26, the hexagonal antiprism (with occupied poles) by 24, and the icosahedron by 20. In each of these, each corner is connected with five or six others that form a nearly planar pentagon or hexagon, respectively. It is possible (Pauling, private communication) that these configurations are more stable than squares because they reduce repulsions that may exist between atoms at nonadjacent corners. With atoms arranged at the distance a at the corners of a square, the next-nearest-neighbor distance is 1.41 a, while in a pentagon it is 1.62 a, and in a hexagon 1.73 a. In a triangular arrangement there are no unbonded neighbors to produce repulsion. In this context it may be of interest to direct attention to Fig. 20 and Figs. 24f and g. Here we observe a pronounced tendency toward the creation of large atom complexes with fivefold axes of symmetry.

A second important factor of triangular configurations is that they are a prerequisite for the formation of tetrahedral interstices; square configurations give rise to octahedral interstices. The volume of a central sphere that touches six contiguous spheres forming an octahedron is 6.3 times larger than a sphere that is at the center of a corresponding tetrahedron. Thus, tetrahedral configurations result in a minimum of interstitial space.

One of the most important factors stabilizing the icosahedral configuration is probably the shortened center-to-vertex distance. The most tangible experimental evidence for the tendency of atoms of unlike atomic radii to arrange themselves into these configurations has been brought forth in βMg_2Al_3. Here, the disorder, which provides the stability, brings about a substantial increase in the number of icosahedral coordination shells, and the apparent requirement is satisfied that about one-half of the vertices should be occupied by large atoms (magnesium) and the other half by small atoms (aluminum). It is possible that other disordered structures, which for a long time have defied detailed analyses, may be attributed to the same cause.

The icosahedron seems to be the one coordination shell that is most preferred in intermetallic compounds.

METALLIC RADII AND ATOMIC SIZES

The metrical properties of the polyhedra so far discussed are clearly inconsistent with sphere packing, as has been shown in the initial sections of this article. We have also seen that the atom

at the center of a Friauf polyhedron (A atom) appears to be tetrahedrally deformed, whereas the μ-phase polyhedron results in trigonal deformation.

The ratio between the distances A-B and B-B = a (a = average edge of the truncated tetrahedra) has the characteristic value of 1.17 that does not change significantly from one Friauf polyhedron to another[6,9,17] or even from one structure type to another, although the nominal radius ratios A/B of the atoms may differ drastically. The most instructive example is αMn, which is isostructural with $\gamma Mg_{17}Al_{12}$; see also Fig. 25a. Here, the nominal radius ratio is unity, but the manganese atoms behave as if they were of drastically different sizes. Of the 58 atoms in the body-centered cubic cell of edge length 8.91Å, ten are inside Friauf polyhedra (large Mn atoms), 24 are at hybrid vertices of the kind shown in Fig. 25a (mode VII, intermediate size), and 24 occupy centers of icosahedra (small Mn atoms).

In αVAl_{10}, which is isostructural with $Mg_3Cr_2Al_{18}$,[19] there are no large atoms (for example, magnesium) to occupy the centers of the Friauf polyhedra, and these are, in fact, empty part of the time.[32] The formula may be written $(Al_2, \text{hole})_3\ V_2Al_{18}$. It can be seen[21] that this phenomenon is explicable on the basis of the VEC rule. In the AB_{22} compounds[20] (Fig. 24d) the B atoms seem to be of drastically different sizes.

Rudman[30] observed that in many structures of the Friauf type (C14 and C15), aluminum behaves as if its atomic size were considerably smaller than in the pure metal, and that this behavior is also reflected in the nature of substitutional solid solutions with aluminum. The Al-Al distances observed in βMg_2Al_3 (and these are extremely numerous) are clearly consistent with this observation, but a still more striking example is found in $Mg_2Cu_6Al_5$.[31] Here, an aluminum atom is at the center of an icosahedron that has twelve copper atoms at the vertices. This arrangement indicates that the effective size of the aluminum atom is about ten per cent smaller than that of the copper atoms, whereas in pure aluminum the metallic "radius" is 12 per cent larger than in pure copper.

The apparently large size of the magnesium atoms inside the Friauf polyhedra in Mg_2Al_3 may be attributed to the fact that two metallic valences are engaged in sixteen bonds, and thus each represents a weak bond that corresponds to a large interatomic distance.

"Metallic radius" or "atomic size" does not seem to represent a meaningful concept unless it is used in connection with terms that describe the conditions under which it is observed, such as the ligancy, bond number, and valence, or perhaps some other important properties that have yet to be defined.

ACKNOWLEDGMENT

Acknowledgment is made to the National Science Foundation for its financial support (Grants GP-1701 and GP-4237), which enabled me to carry out the investigations described here.

REFERENCES

1. L. Pauling, J. Am. Chem. Soc. 45: 2777, 1923.
2. L. Pauling, Am. Sci. 43: 285, 1955.
3. H. Perlitz, Nature (London) 154: 607, 1944.
4. H. Perlitz, Chalmers Tekniska Högskolas Handlingar 50: 1, 1946.
5. F. Laves and K. Möller, Z. Metallk. 30: 232, 1938.
6. S. Samson, Acta Cryst. 23: 586, 1967.
7. R. Borg, AIME Trans. 221: 527, 1961.
8. E. A. Owen and L. Pickup, Proc. Roy. Soc. (London) A139: 526, 1933.
9. S. Samson, Acta Cryst. 19: 401, 1965.
10. J. B. Friauf, J. Am. Chem. Soc. 49: 3107, 1927.
11. J. B. Friauf, Phys. Rev. 29: 34, 1927.
12. F. Laves and H. Witte, Metallwirt. 14: 645, 1935.
13. H. Arnfelt and A. Westgren, Jernkontor. Ann. 119: 185, 1935.
14. D. P. Shoemaker, C. B. Shoemaker, and F. C. Wilson, Acta Cryst. 10: 1, 1957.
15. S. Samson, Nature (London) 195: 259, 1962.
16. F. Laves, K. Löhberg, and P. Rahlfs, Nach. Ges. Wiss. Göttingen, Fachgr. IV 1: 67, 1934.
17. S. Samson and E. K. Gordon, Acta Cryst. B24: 1004, 1968.
18. S. Samson, Acta Cryst. 17: 491, 1964.
19. S. Samson, Acta Cryst. 11: 851, 1958.
20. S. Samson, Acta Cryst. 14: 1229, 1961.
21. S. Samson, Chapter in book; "Structural Chemistry and Molecular Biology", W. H. Freeman and Company, San Francisco, 1968, pp. 687-717.
22. Y. Komura, Acta Cryst. 15: 770, 1962.
23. C. B. Shoemaker and D. P. Shoemaker, Acta Cryst. 16: 997, 1963.
24. P. J. Brown, Acta Cryst. 10: 133, 1957.

25. A. J. Bradley and J. Thewlis, Proc. Roy. Soc. (London) A115: 456, 1927.

26. J. S. Kasper, Acta Met. 2: 456, 1954.

27. Y. Komura, W. G. Sly, and D. P. Shoemaker, Acta Cryst. 13: 575, 1960.

28. G. Bergman, L. T. Waugh, and L. Pauling, Acta Cryst. 10: 254, 1957.

29. E. D. Sands, Q. C. Johnson, A. Zalkin, O. H. Krikorian, and K. L. Kromholtz, Acta Cryst. 15: 832, 1962.

30. R. S. Rudman, AIME Trans. 233: 874, 1965.

31. S. Samson, Acta Chem. Scand. 3: 809, 1949.

32. A. E. Ray and J. F. Smith, Acta Cryst. 10: 604, 1957.

33. J. B. Clark and F. N. Rhines, AIME Trans. J. Metals 2: 6, 1957.